

On frequency- and time-limited \mathcal{H}_2 -optimal model order reduction

Umair Zulfiqar^a, Victor Sreeram^a, and Xin Du^{b,c,d}

^aSchool of Electrical, Electronics and Computer Engineering, The University of Western Australia (UWA), Perth, Australia; ^bSchool of Mechatronic Engineering and Automation, and Shanghai Key Laboratory of Power Station Automation Technology, Shanghai University, Shanghai, China; ^cKey Laboratory of Knowledge Automation for Industrial Processes, Ministry of Education, Beijing, China; ^dKey Laboratory of Modern Power System Simulation and Control & Renewable Energy Technology, Ministry of Education (Northeast Electric Power University), Jilin, China

ARTICLE HISTORY

Compiled September 15, 2021

ABSTRACT

In this paper, the problems of frequency-limited and time-limited \mathcal{H}_2 -optimal model order reduction of linear time-invariant systems are considered within the oblique projection framework. It is shown that it is inherently not possible to satisfy all the necessary conditions for the local minimizer in the oblique projection framework. The conditions for exact satisfaction of the optimality conditions are also discussed. Further, the equivalence between the tangential interpolation conditions and the gramians-based necessary condition for the local optimum is established. Based on this equivalence, iterative algorithms that nearly satisfy these interpolation-based necessary conditions are proposed. The deviation in satisfaction of the optimality conditions decay as the order of the reduced-model is increased in the proposed algorithms. Moreover, stationary point iteration algorithms that satisfy two out of three necessary conditions for the local minimizer are also proposed. There also, the deviation in satisfaction of the third optimality conditions decay as the order of the reduced-model is increased in the proposed algorithms. The efficacy of the proposed algorithms is validated by considering one illustrative and three high-order models that are considered a benchmark for testing model order reduction algorithms.

KEYWORDS

\mathcal{H}_2 -optimal; frequency-limited; model order reduction; near-optimal; oblique projection; pseudo-optimal; reduced-order modeling; suboptimal; time-limited

1. Introduction

The behaviour of the dynamic systems is expressed as mathematical models comprising of several differential equations. The complexity of modern-day dynamic systems has been increasing at a rapid pace due to scientific innovation and sophistication, resulting in large-scale models, which comprise thousands of differential equations. These models are difficult to simulate and analyze due to the excessive computational demand posed by them. The design procedures, which take these models as input, often end up giving complex solutions that are practically not feasible for implementation. To overcome this challenge, model order reduction (MOR) procedures are used to obtain a reduced-

order approximation of the original model. The reduced-order model (ROM) can serve as a surrogate for the original model as its behaviour is close to that of the original model, but it is cheaper to simulate and analyze. The design procedures are also simplified with an admissible numerical accuracy by using the ROMs as surrogates for the original high-order model (Benner et al., 2005; Schilders et al., 2008). The MOR procedure should preserve important characteristics and properties of the original model. The specific characteristics to be preserved in the ROM lead to various families of MOR algorithms (Benner, 2018; Quarteroni et al., 2014).

The performance of a MOR procedure is judged by computing various system norms of the error transfer function. The \mathcal{H}_∞ norm and the \mathcal{H}_2 norm are most widely used as they depict the worst-case scenarios (Zhou et al., 1996). The \mathcal{H}_∞ norm is a more important norm from a system theory perspective as several performance measures in control and communication systems are expressed in terms of the \mathcal{H}_∞ norm (Wolf, 2014). However, the efficient computation of the \mathcal{H}_∞ is a challenge in a large-scale setting. Further, the MOR algorithms that tend to ensure less \mathcal{H}_∞ are generally computationally expensive. In particular, an optimal ROM in the \mathcal{H}_∞ is hard to find, and the algorithms available are computationally demanding (Castagnotto et al., 2017). The MOR procedure should not be a computational challenge in itself; instead, it should reduce the computational cost of the overall experiment. The \mathcal{H}_2 norm, on the other hand, can be computed efficiently due to its relation with the system gramians (Zhou et al., 1996). There are several low-rank methods to efficiently compute these gramians in a large-scale setting (Gugercin et al., 2003; Li and White, 2002; Penzl, 1999), which makes the \mathcal{H}_2 norm a popular choice for assessing the quality of the ROM. Moreover, there exist several algorithms that compute an optimal ROM in the \mathcal{H}_2 norm cheaply in a large-scale setting (Gugercin et al., 2008; Van Dooren et al., 2008; Xu and Zeng, 2011). Therefore, we also have used the \mathcal{H}_2 norm of the error transfer function as a performance measure for the MOR in this paper.

The \mathcal{H}_2 -optimal MOR problem is to find a local optimum for the (squared) \mathcal{H}_2 norm of the error transfer function. The interpolation-based algorithm that computes a local optimum for single-input single-output (SISO) systems was first proposed in (Gugercin et al., 2008), which was later generalized for multi-input multi-output (MIMO) systems in (Van Dooren et al., 2008). A more general algorithm based on Sylvester equations was presented in (Xu and Zeng, 2011), which was further improved in (Benner et al., 2011). These algorithms are iterative algorithms with no guarantee of convergence. Generally, these algorithms quickly converge for SISO systems, but the convergence slows down as the number of inputs and outputs increases in MIMO systems. Some trust region-based methods to speed up convergence in these methods are also reported in the literature like the one in (Beattie and Gugercin, 2009).

Some suboptimal methods for MOR in the \mathcal{H}_2 norm are also reported in the literature that satisfy a subset of the optimality conditions while preserving some additional properties like stability, cf. (Gugercin, 2008; Ibrir, 2018; Wolf et al., 2013). Unlike the algorithm in (Gugercin, 2008), the pseudo-optimal rational Krylov (PORK) algorithm (Wolf et al., 2013) is not an iterative algorithm, and it generates the ROM in a single run. Moreover, unlike the algorithm in (Ibrir, 2018), PORK does not require the solution of any linear matrix inequality (LMI) to satisfy a subset of the optimality conditions. The stability of the ROM in PORK is not only guaranteed, but it has pole-placement property, i.e., the user can select the location of poles on the ROM.

The frequency- and time-limited MOR problems were first introduced in (Gawronski and Juang, 1990). In these problems, it is aimed to achieve superior accuracy in the frequency and time intervals specified by the user. Since no practical system or simu-

lation is run over infinite frequency and time ranges, the frequency- and time-limited MOR problems are important problems. Thus several algorithms in this category are reported in the literature like (Du and Yang, 2010; Kürschner, 2018; Li et al., 2014; Tahavori and Shaker, 2013).

Recently, the \mathcal{H}_2 -optimal MOR in limited frequency and time intervals has received a lot of attention. For the frequency-limited \mathcal{H}_2 -optimal MOR problem, the gramian-based optimality conditions are derived in (Petersson, 2013), and the interpolation-based optimality conditions are derived in (Vuillemin, 2014). Similarly, for the time-limited \mathcal{H}_2 -optimal MOR problem, the gramians-based optimality conditions are derived in (Goyal and Redmann, 2019), and the interpolation-based optimality conditions are derived in (Sinani and Gugercin, 2019). The first group of algorithms, in the category of \mathcal{H}_2 -optimal MOR in limited frequency and time intervals, are the nonlinear optimization-based algorithms reported in (Petersson and Löfberg, 2014; Sinani and Gugercin, 2019; Vuillemin, 2014). These algorithms are applicable to the order of few hundreds, after which, they become computationally infeasible. The second group comprises heuristic generalizations of the standard \mathcal{H}_2 -optimal MOR algorithms reported in (Vuillemin et al., 2013) and (Goyal and Redmann, 2019). These algorithms are computationally efficient, but they do not satisfy any optimality conditions. The third group comprises suboptimal MOR algorithms reported in (Zulficar et al., 2019, 2020a,b) that satisfy a subset of the optimality conditions. Unlike the first group, the second and third groups are the oblique projection-based algorithms.

In this paper, we further advance the oblique projection-based framework for the \mathcal{H}_2 -optimal MOR in limited frequency and time intervals. We show that it is inherently not possible to satisfy the complete set of optimality conditions within the oblique projection framework. Further, we show that the heuristic generalizations of standard \mathcal{H}_2 -optimal MOR algorithms reported in (Vuillemin et al., 2013) and (Goyal and Redmann, 2019) nearly satisfy the optimality conditions. The deviations in satisfaction of the optimality conditions decay with an increase in the order of the ROM. The equivalence between the gramians-based conditions in (Goyal and Redmann, 2019) and the interpolation-based conditions in (Sinani and Gugercin, 2019) is also established. Further, iterative tangential interpolation algorithms for both the frequency-limited and time-limited MOR problems are proposed that nearly satisfy the optimality conditions upon convergence. Stationary point algorithms for both the frequency-limited and time-limited MOR problems are proposed that achieve a subset of the optimality conditions upon convergence. The efficacy of the proposed algorithms is demonstrated by using illustrative and benchmark numerical examples. The numerical simulation confirms the significance of the algorithms and theoretical results presented in the paper.

2. Preliminaries

This section covers the preliminary details of the \mathcal{H}_2 -optimal MOR in limited frequency and time intervals. The mathematical notations used throughout the text are given in Table 1.

Table 1.: Mathematical Notations

Notation	Meaning
$[\cdot]^*$	Hermitian
$tr(\cdot)$	Trace
$\mathcal{L}[\cdot]$	Fréchet derivative of the matrix logarithm.
$Ran(\cdot)$	Range
$orth(\cdot)$	Orthogonal basis
$span \{ \cdot \}_{i=1, \dots, r}$	Span of the set of r vectors

2.1. Problem setting

Let $G(s)$ be an n^{th} -order $p \times m$ transfer function of a stable linear time-invariant system, which is related to its state-space realization (A, B, C) as

$$G(s) = C(sI - A)^{-1}B$$

where $A \in \mathbb{R}^{n \times n}$, $B \in \mathbb{R}^{n \times m}$, and $C \in \mathbb{R}^{p \times n}$. The state-space equations of this realization are given as

$$\dot{x}(t) = Ax(t) + Bu(t), \quad y(t) = Cx(t).$$

The MOR problem is to construct an r^{th} -order $p \times m$ transfer function $\hat{G}(s)$ that closely approximates $G(s)$ where $r \ll n$. Let $\hat{G}(s)$ be related to its state-space realization $(\hat{A}, \hat{B}, \hat{C})$ as

$$\hat{G}(s) = \hat{C}(sI - \hat{A})^{-1}\hat{B}$$

where $\hat{A} \in \mathbb{R}^{r \times r}$, $\hat{B} \in \mathbb{R}^{r \times m}$, and $\hat{C} \in \mathbb{R}^{p \times r}$. The state-space equations of this realization are given as

$$\dot{x}_r(t) = \hat{A}x_r(t) + \hat{B}u(t), \quad y_r(t) = \hat{C}x_r(t).$$

Let $\hat{V} \in \mathbb{R}^{n \times r}$ and $\hat{W} \in \mathbb{R}^{n \times r}$ be the input and output reduction matrices, respectively, which project $G(s)$ onto an r -dimensional subspace where $\Pi = \hat{V}\hat{W}^T$ is the oblique projection, $\hat{W}^T\hat{V} = I$, and the columns of \hat{V} span the reduced subspace along the kernel of \hat{W}^T . The r^{th} -order ROM obtained via projection is given as

$$\hat{A} = \hat{W}^T A \hat{V}, \quad \hat{B} = \hat{W}^T B, \quad \hat{C} = C \hat{V}. \quad (1)$$

The error transfer function $E(s) = G(s) - \hat{G}(s)$ has the following equivalence with its state-space realization (A_e, B_e, C_e)

$$E(s) = C_e(sI - A_e)^{-1}B_e$$

where

$$A_e = \begin{bmatrix} A & 0 \\ 0 & \hat{A} \end{bmatrix}, \quad B_e = \begin{bmatrix} B \\ \hat{B} \end{bmatrix}, \quad C_e = [C \quad -\hat{C}].$$

Let $P_{e,\omega}$ and $Q_{e,\omega}$ be the frequency-limited controllability and the frequency-limited observability gramians, respectively, of the realization (A_e, B_e, C_e) within the frequency interval $[-\omega, \omega]$ rad/sec (Gawronski and Juang, 1990), which solve the following Lyapunov equations

$$\begin{aligned} A_e P_{e,\omega} + P_{e,\omega} A_e^T + B_{e,\omega} B_{e,\omega}^T + B_e B_{e,\omega}^T &= 0, \\ A_e^T Q_{e,\omega} + Q_{e,\omega} A_e + C_{e,\omega}^T C_e + C_e^T C_{e,\omega} &= 0 \end{aligned}$$

where

$$\begin{aligned} B_{e,\omega} &= F_\omega[A_e]B_e, & C_{e,\omega} &= C_e F_\omega[A_e], \\ F_\omega[A_e] &= \frac{j}{2\pi} \log((j\omega I + A_e)(-j\omega I + A_e)^{-1}). \end{aligned}$$

The energy of the impulse response of $E(s)$ within the frequency interval $[-\omega, \omega]$ rad/sec is quantified by the frequency-limited \mathcal{H}_2 -norm (Petersson and Löffberg, 2014), which is related to $P_{e,\omega}$ and $Q_{e,\omega}$ as

$$\begin{aligned} \|E(s)\|_{\mathcal{H}_{2,\omega}} &= \sqrt{\text{tr}(C_e P_{e,\omega} C_e^T)} = \sqrt{\text{tr}(C P_\omega C^T - 2C \bar{P}_\omega \hat{C}^T + \hat{C} \hat{P}_\omega \hat{C}^T)} \\ &= \sqrt{\text{tr}(B_e^T Q_{e,\omega} B_e)} = \sqrt{\text{tr}(B^T Q_\omega B - 2B^T \bar{Q}_\omega \hat{B} + \hat{B}^T \hat{Q}_\omega \hat{B})}. \end{aligned}$$

$P_\omega, Q_\omega, \bar{P}_\omega, \bar{Q}_\omega, \hat{P}_\omega,$ and \hat{Q}_ω solve the following linear matrix equations

$$A P_\omega + P_\omega A^T + B B_\omega^T + B_\omega B^T = 0, \quad (2)$$

$$A^T Q_\omega + Q_\omega A + C^T C_\omega + C_\omega^T C = 0, \quad (3)$$

$$A \bar{P}_\omega + \bar{P}_\omega \hat{A}^T + B \hat{B}_\omega^T + B_\omega \hat{B}^T = 0, \quad (4)$$

$$A^T \bar{Q}_\omega + \bar{Q}_\omega \hat{A} + C^T \hat{C}_\omega + C_\omega^T \hat{C} = 0, \quad (5)$$

$$\hat{A} \hat{P}_\omega + \hat{P}_\omega \hat{A}^T + \hat{B} \hat{B}_\omega^T + \hat{B}_\omega \hat{B}^T = 0, \quad (6)$$

$$\hat{A}^T \hat{Q}_\omega + \hat{Q}_\omega \hat{A} + \hat{C}^T \hat{C}_\omega + \hat{C}_\omega^T \hat{C} = 0 \quad (7)$$

where

$$B_\omega = F_\omega[A]B, \quad \hat{B}_\omega = F_\omega[\hat{A}]\hat{B}, \quad C_\omega = C F_\omega[A], \quad \hat{C}_\omega = \hat{C} F_\omega[\hat{A}].$$

In the frequency-limited MOR problem, the frequency response of $E(s)$ is sought to be small within the desired frequency interval $\Omega = [-\omega, \omega]$ rad/sec, which is generally quantified by the $\mathcal{H}_{2,\omega}$ -norm. Thus the $\mathcal{H}_{2,\omega}$ -MOR problem under consideration is to construct $\hat{G}(s)$ such that $\|E(s)\|_{\mathcal{H}_{2,\omega}}$ is small, i.e.,

$$\min_{\substack{\hat{G}(s) \\ \text{order}=r}} \|E(s)\|_{\mathcal{H}_{2,\omega}}.$$

This, in turn, ensures that $\|Y(\nu) - Y_r(\nu)\|$ is small within the desired frequency interval $\Omega = [-\omega, \omega]$ rad/sec where $Y(\nu)$ and $Y_r(\nu)$ are the Fourier transforms of $y(t)$ and $y_r(t)$, respectively.

Let $P_{e,\tau}$ and $Q_{e,\tau}$ be the time-limited controllability and the time-limited observability gramians, respectively, of the realization (A_e, B_e, C_e) within the time interval $\mathcal{T} = [0, \tau]$ sec (Gawronski and Juang, 1990), which solve the following Lyapunov equations

$$\begin{aligned} A_e P_{e,\tau} + P_{e,\tau} A_e^T + B_e B_e^T - B_{e,\tau} B_{e,\tau}^T &= 0, \\ A_e^T Q_{e,\tau} + Q_{e,\tau} A_e + C_e^T C_e - C_{e,\tau}^T C_{e,\tau} &= 0. \end{aligned}$$

where

$$B_{e,\tau} = e^{A_e \tau} B_e \quad \text{and} \quad C_{e,\tau} = C_e e^{A_e \tau}.$$

The energy of the impulse response of $E(s)$ within the time interval $\mathcal{T} = [0, \tau]$ sec is quantified by the time-limited \mathcal{H}_2 -norm (Goyal and Redmann, 2019), which is related to $P_{e,\tau}$ and $Q_{e,\tau}$ as

$$\begin{aligned} \|E(s)\|_{\mathcal{H}_{2,\tau}} &= \sqrt{\text{tr}(C_e P_{e,\tau} C_e^T)} = \sqrt{\text{tr}(C P_\tau C^T - 2C \bar{P}_\tau \hat{C}^T + \hat{C} \hat{P}_\tau \hat{C}^T)} \\ &= \sqrt{\text{tr}(B_e^T Q_{e,\tau} B_e)} = \sqrt{\text{tr}(B^T Q_\tau B - 2B^T \bar{Q}_\tau \hat{B} + \hat{B}^T \hat{Q}_\tau \hat{B})}. \end{aligned}$$

$P_\tau, Q_\tau, \bar{P}_\tau, \bar{Q}_\tau, \hat{P}_\tau,$ and \hat{Q}_τ solve the following linear matrix equations

$$A P_\tau + P_\tau A^T + B B^T - B_\tau B_\tau^T = 0, \quad (8)$$

$$A^T Q_\tau + Q_\tau A + C^T C - C_\tau^T C_\tau = 0, \quad (9)$$

$$A \bar{P}_\tau + \bar{P}_\tau \hat{A}^T + B \hat{B}^T - B_\tau \hat{B}_\tau^T = 0, \quad (10)$$

$$A^T \bar{Q}_\tau + \bar{Q}_\tau \hat{A} + C^T \hat{C} - C_\tau^T \hat{C}_\tau = 0 \quad (11)$$

$$\hat{A} \hat{P}_\tau + \hat{P}_\tau \hat{A}^T + \hat{B} \hat{B}^T - \hat{B}_\tau \hat{B}_\tau^T = 0, \quad (12)$$

$$\hat{A}^T \hat{Q}_\tau + \hat{Q}_\tau \hat{A} + \hat{C}^T \hat{C} - \hat{C}_\tau^T \hat{C}_\tau = 0 \quad (13)$$

where

$$B_\tau = e^{A \tau} B, \quad \hat{B}_\tau = e^{\hat{A} \tau} \hat{B}, \quad C_\tau = C e^{A \tau}, \quad \hat{C}_\tau = \hat{C} e^{\hat{A} \tau}.$$

In the time-limited MOR problem, the time response of $E(s)$ is sought to be small within the desired time interval $\mathcal{T} = [0, \tau]$ sec. This is generally quantified by the $\mathcal{H}_{2,\tau}$ -norm. Thus the $\mathcal{H}_{2,\tau}$ -MOR problem under consideration is to construct $\hat{G}(s)$ such that $\|E(s)\|_{\mathcal{H}_{2,\tau}}$ is small, i.e.,

$$\min_{\substack{\hat{G}(s) \\ \text{order}=r}} \|E(s)\|_{\mathcal{H}_{2,\tau}}.$$

This, in turn, ensures that $\|y(t) - y_r(t)\|$ is small within the desired time interval $\mathcal{T} = [0, \tau]$ sec.

2.2. Necessary conditions for the local minimizer

Let \hat{Q} be the observability gramian of the pair (\hat{A}, \hat{C}) , and \bar{Q} solve the following Sylvester equation

$$A^T \bar{Q} + \bar{Q} \hat{A} + C^T \hat{C} = 0.$$

Then the local minimizer $(\hat{A}, \hat{B}, \hat{C})$ for $\|E(s)\|_{\mathcal{H}_{2,\omega}}^2$ satisfies the following gramian-based conditions (Petersson and Löfberg, 2014)

$$\bar{Q}^T \bar{P}_\omega - \hat{Q} \hat{P}_\omega + Z_\omega = 0, \quad (14)$$

$$\bar{Q}_\omega^T B - \hat{Q}_\omega \hat{B} = 0, \quad (15)$$

$$C \bar{P}_\omega - \hat{C} \hat{P}_\omega = 0 \quad (16)$$

where

$$Z_\omega = \operatorname{Re} \left(\frac{j}{\pi} \mathcal{L}(-\hat{A} - j\omega I, \hat{C}^T \hat{C} \hat{P}_\omega - \hat{C}^T C \bar{P}_\omega) \right).$$

Let $G(s)$ and $\hat{G}(s)$ have simple poles and the following pole-residue forms

$$G(s) = \sum_{i=1}^n \frac{l_i r_i^T}{s - \lambda_i}, \quad \hat{G}(s) = \sum_{i=1}^r \frac{\hat{l}_i \hat{r}_i^T}{s - \hat{\lambda}_i}.$$

Now define $G_\omega(s)$, $T_\omega(s)$, $\hat{G}_\omega(s)$ and $\hat{T}_\omega(s)$ as

$$G_\omega(s) = \sum_{i=1}^n \frac{l_i r_i^T}{s - \lambda_i} F_\omega[\lambda_i], \quad T_\omega(s) = G_\omega(s) + G(s) F_\omega[-s],$$

$$\hat{G}_\omega(s) = \sum_{i=1}^r \frac{\hat{l}_i \hat{r}_i^T}{s - \hat{\lambda}_i} F_\omega[\hat{\lambda}_i], \quad \hat{T}_\omega(s) = \hat{G}_\omega(s) + \hat{G}(s) F_\omega[-s].$$

Then the local minimizer $\hat{G}(s)$ for $\|E(s)\|_{\mathcal{H}_{2,\omega}}^2$ satisfies the following bi-tangential Hermite interpolation conditions (Vuillemin, 2014)

$$\tilde{l}_i^T T_\omega'(-\hat{\lambda}_i) \hat{r}_i = \tilde{l}_i^T \hat{T}_\omega'(-\hat{\lambda}_i) \hat{r}_i, \quad (17)$$

$$\tilde{l}_i^T T_\omega(-\hat{\lambda}_i) = \tilde{l}_i^T \hat{T}_\omega(-\hat{\lambda}_i), \quad (18)$$

$$T_\omega(-\hat{\lambda}_i) \hat{r}_i = \hat{T}_\omega(-\hat{\lambda}_i) \hat{r}_i. \quad (19)$$

Similarly, the local minimizer $(\hat{A}, \hat{B}, \hat{C})$ for $\|E(s)\|_{\mathcal{H}_{2,\tau}}^2$ satisfies the following gramians-based conditions (Goyal and Redmann, 2019)

$$\bar{Q}^T \bar{P}_\tau - \hat{Q} \hat{P}_\tau + Z_\tau = 0, \quad (20)$$

$$\bar{Q}_\tau^T B - \hat{Q}_\tau \hat{B} = 0, \quad (21)$$

$$C \bar{P}_\tau - \hat{C} \hat{P}_\tau = 0 \quad (22)$$

where

$$Z_\tau = \tau(\hat{Q}e^{\hat{A}\tau}\hat{B}\hat{B}^Te^{\hat{A}^T\tau} - \bar{Q}^Te^{A\tau}B\hat{B}^Te^{\hat{A}^T\tau}).$$

Assuming that $G(s)$ and $\hat{G}(s)$ have simple poles, define $G_\tau(s)$, $T_\tau(s)$, $\hat{G}_\tau(s)$, and $\hat{T}_\tau(s)$ as

$$\begin{aligned} G_\tau(s) &= -e^{-s\tau}C(sI - A)^{-1}e^{A\tau}B, & T_\tau(s) &= G_\tau(s) + G(s), \\ \hat{G}_\tau(s) &= -e^{-s\tau}\hat{C}(sI - \hat{A})^{-1}e^{\hat{A}\tau}\hat{B}, & \hat{T}_\tau(s) &= \hat{G}_\tau(s) + \hat{G}(s). \end{aligned}$$

Then the local minimizer $\hat{G}(s)$ for $\|E(s)\|_{\mathcal{H}_{2,\tau}}^2$ satisfies the following bi-tangential Hermite interpolation conditions (Sinani and Gugercin, 2019)

$$\tilde{l}_i^T T'_\tau(-\hat{\lambda}_i)\hat{r}_i = \tilde{l}_i^T \hat{T}'_\tau(-\hat{\lambda}_i)\hat{r}_i, \quad (23)$$

$$\tilde{l}_i^T T_\tau(-\hat{\lambda}_i) = \tilde{l}_i^T \hat{T}_\tau(-\hat{\lambda}_i), \quad (24)$$

$$T_\tau(-\hat{\lambda}_i)\hat{r}_i = \hat{T}_\tau(-\hat{\lambda}_i)\hat{r}_i. \quad (25)$$

3. Existing oblique projection-based MOR techniques

In this section, some important oblique projection-based algorithms for the $\mathcal{H}_{2,\omega}$ - and $\mathcal{H}_{2,\tau}$ -MOR problems are briefly reviewed.

3.1. Frequency-limited two-sided iteration algorithm (FLTSIA)

FLTSIA (Du et al., 2021; Vuillemin et al., 2013) is a heuristic generalization of (Xu and Zeng, 2011) based on analogy and experimental results. Starting with an initial guess of the ROM, the reduction matrices are updated as $\hat{V} = \bar{P}_\omega$ and $\hat{W} = \bar{Q}_\omega$. To ensure the oblique projection condition $\hat{W}^T\hat{V} = I$, the correction equation $\hat{W} = \hat{W}(\hat{V}^T\hat{W})^{-1}$ is used. The ROM is generated by using these reduction matrices, and the process is repeated until the algorithm converges. It will be shown later in this paper that the ROM constructed by FLTSIA does not satisfy the optimality conditions (14)-(16), in general.

3.2. Frequency-limited pseudo-optimal rational Krylov algorithm (FLPORK)

Let us define B_Ω , C_Ω , \hat{B}_Ω , and \hat{C}_Ω as

$$\begin{aligned} B_\Omega &= [B \quad B_\omega], & C_\Omega &= \begin{bmatrix} C \\ C_\omega \end{bmatrix}, \\ \hat{B}_\Omega &= [\hat{B} \quad \hat{B}_\omega], & \hat{C}_\Omega &= \begin{bmatrix} \hat{C} \\ \hat{C}_\omega \end{bmatrix}. \end{aligned}$$

Now define $G_\Omega(s)$, $\hat{G}_\Omega(s)$, $H_\Omega(s)$, and $\hat{H}_\Omega(s)$ as

$$\begin{aligned} G_\Omega(s) &= C(sI - A)^{-1}B_\Omega, & \hat{G}_\Omega(s) &= \hat{C}(sI - \hat{A})^{-1}\hat{B}_\Omega, \\ H_\Omega(s) &= C_\Omega(sI - A)^{-1}B, & \hat{H}_\Omega(s) &= \hat{C}_\Omega(sI - \hat{A})^{-1}\hat{B}. \end{aligned}$$

Assuming that $G(s)$ and $\hat{G}(s)$ have simple poles, it is shown in (Zulfiqar et al., 2020a) that when $\hat{G}(s)$ satisfies the following tangential interpolation conditions

$$\bar{l}_i^T H_\Omega(-\hat{\lambda}_i) = \bar{l}_i^T \hat{H}_\Omega(-\hat{\lambda}_i), \quad (26)$$

$$G_\Omega(-\hat{\lambda}_i)\bar{r}_i = \hat{G}_\Omega(-\hat{\lambda}_i)\bar{r}_i \quad (27)$$

where $\bar{l}_i = \begin{bmatrix} F_\omega[\hat{\lambda}_i]\hat{l}_i \\ \hat{l}_i \end{bmatrix}$ and $\bar{r}_i = \begin{bmatrix} F_\omega[\hat{\lambda}_i]\hat{r}_i \\ \hat{r}_i \end{bmatrix}$, the optimality conditions (15) and (16) are respectively satisfied. The input reduction matrix \hat{V} in FLPORK (Zulfiqar et al., 2020a) is obtained as

$$\text{Ran}(\hat{V}) = \text{span} \left\{ (\hat{\sigma}_i I - A)^{-1} B_\Omega \bar{b}_i \right\}_{i=1, \dots, r} \quad (28)$$

where $\hat{\sigma}_i$ is the interpolation point, \hat{b}_i is the right tangential direction, and $\bar{b}_i = \begin{bmatrix} F_\omega[-\hat{\sigma}_i]\hat{b}_i \\ \hat{b}_i \end{bmatrix}$. Now define the oblique projection $\Pi = \hat{V}\hat{W}^T$ wherein \hat{W} is arbitrary. Also, define B_\perp , \hat{S} , and \bar{L} as

$$B_\perp = (I - \Pi)B_\Omega, \quad \bar{L} = (B_\perp^T B_\perp)^{-1} B_\perp (I - \Pi)A\hat{V} \quad \hat{S} = \hat{W}^T (A\hat{V} - B_\Omega \bar{L}).$$

Further, partition \bar{L} as $\bar{L} = \begin{bmatrix} \hat{L}_\omega \\ \hat{L} \end{bmatrix}$ where $\hat{L}_\omega = \hat{L}F_\omega[-\hat{S}]$. The frequency-limited observability gramian $\hat{Q}_{s,\omega}$ of the pair $(-\hat{S}, \hat{L})$ solves the following Lyapunov equation

$$-\hat{S}^T \hat{Q}_{s,\omega} - \hat{Q}_{s,\omega} \hat{S} + \hat{L}^T \hat{L}_\omega + \hat{L}_\omega^T \hat{L} = 0.$$

Then $\hat{G}(s)$ that satisfies the optimality condition (16) can be obtained as

$$\hat{A} = -\hat{Q}_{s,\omega}^{-1} \hat{S}^T \hat{Q}_{s,\omega}, \quad \hat{B} = -\hat{Q}_{s,\omega}^{-1} \hat{L}^T, \quad \hat{C} = C\hat{V}.$$

A dual result also exists that constructs a ROM, which satisfies the optimality condition (15). The output reduction matrix \hat{W} in this case is obtained as

$$\text{Ran}(\hat{W}) = \text{span} \left\{ (\hat{\sigma}_i I - A)^{-T} C_\Omega^T \bar{c}_i^T \right\}_{i=1, \dots, r} \quad (29)$$

where \hat{c}_i is the left tangential direction and $\bar{c}_i = \begin{bmatrix} F_\omega[-\hat{\sigma}_i]\hat{c}_i & \hat{c}_i \end{bmatrix}$. Now define the oblique projection $\Pi = \hat{V}\hat{W}^T$ wherein \hat{V} is arbitrary. Also, define C_\perp , \bar{L} , and \hat{S} as

$$C_\perp = C_\Omega(I - \Pi), \quad \bar{L} = \hat{W}^T A(I - \Pi)C_\perp^T (C_\perp C_\perp^T)^{-1}, \quad \hat{S} = (\hat{W}^T A - \bar{L}C_\Omega)\hat{V}.$$

Further, partition \bar{L} as $\bar{L} = [\hat{L}_\omega \quad \hat{L}]$ where $\hat{L}_\omega = F_\omega[-\hat{S}]\hat{L}$. The frequency-limited controllability gramian $\hat{P}_{s,\omega}$ of the pair $(-\hat{S}, \hat{L})$ solves the following Lyapunov equation

$$-\hat{S}\hat{P}_{s,\omega} - \hat{P}_{s,\omega}\hat{S}^T + \hat{L}_\omega\hat{L}^T + \hat{L}\hat{L}_\omega^T = 0.$$

Then $\hat{G}(s)$ that satisfies the optimality condition (15) can be obtained as

$$\hat{A} = -\hat{P}_{s,\omega}\hat{S}^T\hat{P}_{s,\omega}^{-1}, \quad \hat{B} = W^T B, \quad \hat{C} = -\hat{L}^T\hat{P}_{s,\omega}^{-1}.$$

Remark 1. It was later identified in (Zulfiqar et al., 2019) that the interpolation conditions (26) and (26) are the necessary conditions for the local optimum and are equivalent to (15) and (16), respectively, when $G(s)$ and $\hat{G}(s)$ have simple poles.

3.3. Time-limited iterative rational Krylov algorithm (TLIRKA)

TLIRKA (Goyal and Redmann, 2019) is a heuristic generalization of the iterative rational Krylov algorithm (IRKA) (Gugercin et al., 2008) for the time-limited case. Let $\hat{G}(s)$ has simple poles and $\hat{A} = \hat{R}\hat{\Lambda}\hat{R}^{-1}$ be the spectral factorization of \hat{A} where $\hat{\Lambda} = \text{diag}(\hat{\lambda}_1, \dots, \hat{\lambda}_r)$. Starting with a random guess of the ROM, the reduction matrices in TLIRKA are computed as $\hat{V} = \bar{P}_\tau\hat{R}^{-*}$ and $\hat{W} = \bar{Q}_\tau\hat{R}$. To ensure the oblique projection condition $\hat{W}^*\hat{V} = I$, \hat{V} and \hat{W} are updated as $\hat{V} = \text{orth}(\hat{V})$, $\hat{W} = \text{orth}(\hat{W})$, and $\hat{W} = \hat{W}(\hat{V}^*\hat{W})^{-1}$. The ROM is generated by using these reduction matrices, and the process is repeated until the algorithm converges. In general, The ROM constructed by TLIRKA does not satisfy the optimality conditions (20)-(22).

3.4. Time-limited pseudo-optimal rational Krylov algorithm (TLPORK)

Let us define $B_\mathcal{T}$, $C_\mathcal{T}$, $\hat{B}_\mathcal{T}$, and $\hat{C}_\mathcal{T}$ as

$$\begin{aligned} B_\mathcal{T} &= [B \quad -B_\tau], & C_\mathcal{T} &= \begin{bmatrix} C \\ -C_\tau \end{bmatrix}, \\ \hat{B}_\mathcal{T} &= [\hat{B} \quad -\hat{B}_\tau], & \hat{C}_\mathcal{T} &= \begin{bmatrix} \hat{C} \\ -\hat{C}_\tau \end{bmatrix}. \end{aligned}$$

Now define $G_\mathcal{T}(s)$, $\hat{G}_\mathcal{T}(s)$, $H_\mathcal{T}(s)$, and $\hat{H}_\mathcal{T}(s)$ as

$$\begin{aligned} G_\mathcal{T}(s) &= C(sI - A)^{-1}B_\mathcal{T}, & \hat{G}_\mathcal{T}(s) &= \hat{C}(sI - \hat{A})^{-1}\hat{B}_\mathcal{T}, \\ H_\mathcal{T}(s) &= C_\mathcal{T}(sI - A)^{-1}B, & \hat{H}_\mathcal{T}(s) &= \hat{C}_\mathcal{T}(sI - \hat{A})^{-1}\hat{B}. \end{aligned}$$

Assuming that $G(s)$ and $\hat{G}(s)$ have simple poles, it is shown in (Zulfiqar et al., 2020b) that $\hat{G}(s)$ satisfies the optimality conditions (21) and (22) if the following tangential interpolation conditions are respectively satisfied

$$\tilde{l}_i^T H_\mathcal{T}(-\hat{\lambda}_i) = \tilde{l}_i^T \hat{H}_\mathcal{T}(-\hat{\lambda}_i), \quad (30)$$

$$G_\mathcal{T}(-\hat{\lambda}_i)\tilde{r}_i = \hat{G}_\mathcal{T}(-\hat{\lambda}_i)\tilde{r}_i \quad (31)$$

where $\tilde{l}_i = \begin{bmatrix} \hat{l}_i \\ e^{\hat{\lambda}_i t} \hat{l}_i \end{bmatrix}$ and $\tilde{r}_i = \begin{bmatrix} \hat{r}_i \\ e^{\hat{\lambda}_i t} \hat{r}_i \end{bmatrix}$. The input reduction matrix \hat{V} in TLORK (Zulficar et al., 2020b) is obtained as

$$\text{Ran}(\hat{V}) = \underset{i=1, \dots, r}{\text{span}} \{(\hat{\sigma}_i I - A)^{-1} B_{\mathcal{T}} \tilde{b}_i\} \quad (32)$$

where $\tilde{b}_i = \begin{bmatrix} \hat{b}_i \\ e^{-\hat{\sigma}_i t} \hat{b}_i \end{bmatrix}$. Now define the oblique projection $\Pi = \hat{V} \hat{W}^T$ wherein \hat{W} is arbitrary. Also, define B_{\perp} , \hat{S} , and \bar{L} as

$$B_{\perp} = (I - \Pi) B_{\mathcal{T}}, \quad \bar{L} = (B_{\perp}^T B_{\perp})^{-1} B_{\perp} (I - \Pi) A \hat{V} \quad \hat{S} = \hat{W}^T (A \hat{V} - B_{\mathcal{T}} \bar{L}).$$

Further, partition \bar{L} as $\bar{L} = \begin{bmatrix} \hat{L} \\ \hat{L}_{\tau} \end{bmatrix}$ where $\hat{L}_{\tau} = \hat{L} e^{-\hat{S} t}$. The time-limited observability gramian $\hat{Q}_{s, \tau}$ of the pair $(-\hat{S}, \hat{L})$ solves the following Lyapunov equation

$$-\hat{S}^T \hat{Q}_{s, \tau} - \hat{Q}_{s, \tau} \hat{S} + \hat{L}^T \hat{L} - \hat{L}_{\tau}^T \hat{L}_{\tau} = 0.$$

Then $\hat{G}(s)$ that satisfies the optimality condition (22) can be obtained as

$$\hat{A} = -\hat{Q}_{s, \tau}^{-1} \hat{S}^T \hat{Q}_{s, \tau}, \quad \hat{B} = -\hat{Q}_{s, \tau}^{-1} \hat{L}^T, \quad \hat{C} = C \hat{V}.$$

A dual result also exists that constructs a ROM, which satisfies the optimality condition (21). The output reduction matrix \hat{W} in this case is obtained as

$$\text{Ran}(\hat{W}) = \underset{i=1, \dots, r}{\text{span}} \{(\hat{\sigma}_i I - A)^{-T} C_{\mathcal{T}}^T \tilde{c}_i\} \quad (33)$$

where \hat{c}_i is the left tangential direction and $\tilde{c}_i = \begin{bmatrix} \hat{c}_i \\ e^{-\hat{\sigma}_i t} \hat{c}_i \end{bmatrix}$. Now define the oblique projection $\Pi = \hat{V} \hat{W}^T$ wherein \hat{V} is arbitrary. Also, define C_{\perp} , \bar{L} , and \hat{S} as

$$C_{\perp} = C_{\mathcal{T}} (I - \Pi), \quad \bar{L} = \hat{W}^T A (I - \Pi) C_{\perp}^T (C_{\perp} C_{\perp}^T)^{-1}, \quad \hat{S} = (\hat{W}^T A - \bar{L} C_{\mathcal{T}}) \hat{V}.$$

Further, partition \bar{L} as $\bar{L} = \begin{bmatrix} \hat{L} \\ \hat{L}_{\tau} \end{bmatrix}$ where $\hat{L}_{\tau} = e^{-\hat{S} t} \hat{L}$. The time-limited controllability gramian $\hat{P}_{s, \tau}$ of the pair $(-\hat{S}, \hat{L})$ solves the following Lyapunov equation

$$-\hat{S} \hat{P}_{s, \tau} - \hat{P}_{s, \tau} \hat{S}^T + \hat{L} \hat{L}^T - \hat{L}_{\tau} \hat{L}_{\tau}^T = 0.$$

Then $\hat{G}(s)$ that satisfies the optimality condition () can be obtained as

$$\hat{A} = -\hat{P}_{s, \tau} \hat{S}^T \hat{P}_{s, \tau}^{-1}, \quad \hat{B} = W^T B, \quad \hat{C} = -\hat{L}^T \hat{P}_{s, \tau}^{-1}.$$

4. $\mathcal{H}_{2, \omega}$ - and $\mathcal{H}_{2, \tau}$ -optimal MOR

In this section, the problems of $\mathcal{H}_{2, \omega}$ - and $\mathcal{H}_{2, \tau}$ -optimal MOR are considered within the oblique projection framework. An inherent difficulty in constructing a local optimum

within the oblique projection framework is discussed. The conditions for exact satisfaction of the optimality conditions are also discussed. Further, the equivalence between some gramians-based and interpolation-based optimality conditions is established.

4.1. Limitation in the oblique projection framework

Before beginning the discussion on an inherent limitation of the oblique projection framework in satisfying the optimality conditions (14)-(16) and (20)-(22), let us represent the optimality conditions (14) and (20) a bit differently so that it resembles Wilson's condition (Wilson, 1970) of the standard \mathcal{H}_2 -optimal MOR case.

Proposition 4.1. *Let $F_\omega[\hat{A}]$ has full rank. Then the optimality condition (14) can be expressed as*

$$\bar{Q}_\omega^T \bar{P}_\omega - \hat{Q}_\omega \hat{P}_\omega + X_\omega = 0$$

where

$$X_\omega = F_\omega[\hat{A}^T]Z_\omega - \bar{Q}^T F_\omega[A]\bar{P}_\omega + \hat{Q}F_\omega[\hat{A}]\hat{P}_\omega.$$

Similarly, the optimality condition (20) can be rewritten as

$$\bar{Q}_\tau^T \bar{P}_\tau - \hat{Q}_\tau \hat{P}_\tau + X_\tau = 0$$

where

$$X_\tau = Z_\tau + e^{\hat{A}^T \tau} \bar{Q}^T e^{A\tau} \bar{P}_\tau - e^{\hat{A}^T \tau} \hat{Q} e^{\hat{A}\tau} \hat{P}_\tau.$$

Proof. Note that

$$\bar{Q}_\omega^T \bar{P}_\omega = (F_\omega[\hat{A}^T] \bar{Q}^T + \bar{Q}^T F_\omega[A]) \bar{P}_\omega \quad \text{and} \quad \hat{Q}_\omega \hat{P}_\omega = (F_\omega[\hat{A}^T] \hat{Q} + \hat{Q} F_\omega[\hat{A}]) \hat{P}_\omega.$$

Thus

$$F_\omega[\hat{A}^T] \bar{Q}^T \bar{P}_\omega = \bar{Q}_\omega^T \bar{P}_\omega - \bar{Q}^T F_\omega[A] \bar{P}_\omega, \tag{34}$$

$$F_\omega[\hat{A}^T] \hat{Q} \hat{P}_\omega = \hat{Q}_\omega \hat{P}_\omega - \hat{Q} F_\omega[\hat{A}] \hat{P}_\omega. \tag{35}$$

By pre-multiplying with $F_\omega[\hat{A}^T]$, the equation (14) becomes

$$F_\omega[\hat{A}^T] \bar{Q}^T \bar{P}_\omega - F_\omega[\hat{A}^T] \hat{Q} \hat{P}_\omega + F_\omega[\hat{A}^T] Z_\omega = 0. \tag{36}$$

Further, by putting (34) and (35), the equation (36) becomes

$$\bar{Q}_\omega^T \bar{P}_\omega - \hat{Q}_\omega \hat{P}_\omega + X_\omega = 0.$$

Similarly, note that

$$\bar{Q}_\tau^T \bar{P}_\tau = (\bar{Q}^T - e^{\hat{A}^T \tau} \bar{Q}^T e^{A\tau}) \bar{P}_\tau \quad \text{and} \quad \hat{Q}_\tau \hat{P}_\tau = (\hat{Q} - e^{\hat{A}^T \tau} \hat{Q} e^{\hat{A}\tau}) \hat{P}_\tau.$$

Thus

$$\bar{Q}^T \bar{P}_\tau = \bar{Q}_\tau^T \bar{P}_\tau + e^{\hat{A}^T \tau} \bar{Q}^T e^{A\tau} \bar{P}_\tau, \quad (37)$$

$$\hat{Q} \hat{P}_\tau = \hat{Q}_\tau \hat{P}_\tau + e^{\hat{A}^T \tau} \hat{Q} e^{\hat{A}\tau} \hat{P}_\tau. \quad (38)$$

By putting (37) and (38), the equation (20) becomes

$$\bar{Q}_\tau^T \bar{P}_\tau - \hat{Q}_\tau \hat{P}_\tau + X_\tau = 0.$$

This completes the proof. \square

Let us assume that \hat{P}_ω and \hat{Q}_ω are invertible. Then the optimal choices of \hat{B} and \hat{C} according to the optimality conditions (15) and (16), respectively, are given by

$$\hat{B} = \hat{Q}_\omega^{-1} \bar{Q}_\omega^T B \quad \text{and} \quad \hat{C} = C \bar{P}_\omega \hat{P}_\omega^{-1}.$$

Similarly, let us assume that \hat{P}_τ and \hat{Q}_τ are invertible. Then the optimal choices of \hat{B} and \hat{C} according to the optimality conditions (21) and (22), respectively, are given by

$$\hat{B} = \hat{Q}_\tau^{-1} \bar{Q}_\tau^T B \quad \text{and} \quad \hat{C} = C \bar{P}_\tau \hat{P}_\tau^{-1}.$$

If ROMs are obtained within the oblique projection framework, the oblique projections for optimal choices \hat{B} and \hat{C} are given by $\Pi = \bar{P}_\omega \hat{P}_\omega^{-1} \hat{Q}_\omega^{-1} \bar{Q}_\omega^T$ (with $\hat{V} = \bar{P}_\omega \hat{P}_\omega^{-1}$ and $\hat{W} = \bar{Q}_\omega \hat{Q}_\omega^{-1}$) and $\Pi = \bar{P}_\tau \hat{P}_\tau^{-1} \hat{Q}_\tau^{-1} \bar{Q}_\tau^T$ (with $\hat{V} = \bar{P}_\tau \hat{P}_\tau^{-1}$ and $\hat{W} = \bar{Q}_\tau \hat{Q}_\tau^{-1}$). Further, since $\hat{W}^T \hat{V} = I$, $\bar{Q}_\omega^T \bar{P}_\omega - \hat{Q}_\omega \hat{P}_\omega = 0$ and $\bar{Q}_\tau^T \bar{P}_\tau - \hat{Q}_\tau \hat{P}_\tau = 0$. Then deviations in the optimal choices of \hat{A} are given by X_ω and X_τ . It can readily be verified that $X_\omega = 0$ when $F_\omega[A] = \hat{V} F_\omega[\hat{A}] \hat{W}^T$ and $\bar{Q} = \hat{W} \hat{Q}$. Similarly, $X_\tau = 0$ when $e^{A\tau} = \hat{V} e^{\hat{A}\tau} \hat{W}^T$ and $\bar{Q} = \hat{W} \hat{Q}$. Note that $\hat{W} \hat{Q}$, $\hat{V} F_\omega[\hat{A}] \hat{W}^T$, and $\hat{V} e^{\hat{A}\tau} \hat{W}^T$ are the oblique projection-based approximations of \bar{Q} , $F_\omega[A]$, and $e^{A\tau}$, respectively (Benner et al., 2016; Kürschner, 2018). Thus $\bar{Q} \neq \hat{W} \hat{Q}$, $F_\omega[A] \neq \hat{V} F_\omega[\hat{A}] \hat{W}^T$, and $e^{A\tau} \neq \hat{V} e^{\hat{A}\tau} \hat{W}^T$, in general. Resultantly, $X_\omega \neq 0$ and $X_\tau \neq 0$, in general. Therefore, it is inherently not possible to obtain an optimal choice of \hat{A} within the oblique projection framework when the optimal choices of \hat{B} and \hat{C} are made.

4.2. Effect of the change of basis

Note that \hat{P}_ω^{-1} and \hat{Q}_ω^{-1} do not change the subspaces but only change the basis of \bar{P}_ω and \bar{Q}_ω in $\hat{V} = \bar{P}_\omega \hat{P}_\omega^{-1}$ and $\hat{W} = \bar{Q}_\omega \hat{Q}_\omega^{-1}$, respectively. Similarly, \hat{P}_τ^{-1} and \hat{Q}_τ^{-1} only change the basis of \bar{P}_τ and \bar{Q}_τ in $\hat{V} = \bar{P}_\tau \hat{P}_\tau^{-1}$ and $\hat{W} = \bar{Q}_\tau \hat{Q}_\tau^{-1}$, respectively (Gallivan et al., 2004). Thus one may think of constructing the ROM using the oblique projections $\Pi = \bar{P}_\omega \bar{Q}_\omega^T$ (as done in FLTSI) and $\Pi = \bar{P}_\tau \bar{Q}_\tau^T$ (as done in TLIRKA). This change of basis is harmless in the standard \mathcal{H}_2 -optimal MOR; see (Benner et al., 2011; Xu and Zeng, 2011), for instance. However, in the frequency- and time-limited cases, this incurs deviations in the optimal choices of \hat{B} and \hat{C} . The next two theorems show that the deviation caused by this change of basis is zero when $F_\omega[A] = \hat{V} F_\omega[\hat{A}] \hat{W}^T$ and $e^{At} = \hat{V} e^{\hat{A}t} \hat{W}^T$, which is not possible in general.

Theorem 4.2. *The ROM $(\hat{A}, \hat{B}, \hat{C})$ obtained by using the oblique projection $\Pi = \bar{P}_\omega \bar{Q}_\omega^T$ (with $\hat{V} = \bar{P}_\omega$ and $\hat{W} = \bar{Q}_\omega$) satisfies the optimality conditions (15) and (16) provided $B_\omega = \hat{V} \hat{B}_\omega$ and $C_\omega = \hat{C}_\omega \hat{W}^T$.*

Proof. By multiplying \hat{W}^T from the left, the equation (4) becomes

$$\hat{W}^T A \bar{P}_\omega + \hat{W}^T \bar{P}_\omega \hat{A}^T + \hat{W}^T B \hat{B}_\omega^T + \hat{W}^T B_\omega \hat{B}^T = 0.$$

Since $\hat{W}^T \hat{V} = I$ and $\hat{W}^T B_\omega = \hat{B}_\omega$,

$$\hat{A} + \hat{A}^T + \hat{B} \hat{B}_\omega^T + \hat{B}_\omega \hat{B}^T = 0.$$

Due to uniqueness, $\hat{P}_\omega = I$ and thus $C \bar{P}_\omega - C \hat{P}_\omega = 0$.

Similarly, by multiplying \hat{V}^T from the left, the equation (5) becomes

$$\hat{V}^T A^T \bar{Q}_\omega + \hat{V}^T \bar{Q}_\omega \hat{A} + \hat{V}^T C^T \hat{C}_\omega + \hat{V}^T C_\omega^T \hat{C} = 0.$$

Since $\hat{V}^T \hat{W} = I$ and $C_\omega \hat{V} = \hat{C}_\omega$,

$$\hat{A}^T + \hat{A} + \hat{C}^T \hat{C}_\omega + \hat{C}_\omega^T \hat{C} = 0.$$

Due to uniqueness, $\hat{Q}_\omega = I$ and thus $\bar{Q}_\omega^T B - \hat{Q}_\omega^T B = 0$. This completes the proof. \square

$\hat{V} \hat{B}_\omega$ and $\hat{C}_\omega \hat{W}^T$ are projection-based approximations of B_ω and C_ω , respectively. Thus $B_\omega \neq \hat{V} \hat{B}_\omega$ and $C_\omega \neq \hat{C}_\omega \hat{W}^T$, in general. The Krylov-subspace based methods to obtain approximations of B_ω and C_ω as $\hat{V} \hat{B}_\omega$ and $\hat{C}_\omega \hat{W}^T$, respectively, can be found in (Benner et al., 2016).

Theorem 4.3. *The ROM $(\hat{A}, \hat{B}, \hat{C})$ obtained by using the oblique projection $\Pi = \bar{P}_\tau \bar{Q}_\tau^T$ (with $\hat{V} = \bar{P}_\tau$ and $\hat{W} = \bar{Q}_\tau$) satisfies the optimality conditions (21) and (22) provided $B_\tau = \hat{V} \hat{B}_\tau$ and $C_\tau = \hat{C}_\tau \hat{W}^T$.*

Proof. By multiplying \hat{W}^T from the left, the equation (10) becomes

$$\hat{W}^T A \bar{P}_\tau + \hat{W}^T \bar{P}_\tau \hat{A}^T + \hat{W}^T B \hat{B}_\tau^T - \hat{W}^T B_\tau \hat{B}_\tau^T = 0.$$

Since $\hat{W}^T \hat{V} = I$ and $\hat{W}^T B_\tau = \hat{B}_\tau$,

$$\hat{A} + \hat{A}^T + \hat{B} \hat{B}_\tau^T - \hat{B}_\tau \hat{B}_\tau^T = 0.$$

Due to uniqueness, $\hat{P}_\tau = I$ and thus $C \bar{P}_\tau - C \hat{P}_\tau = 0$.

Similarly, by multiplying \hat{V}^T from the left, the equation (11) becomes

$$\hat{V}^T A^T \bar{Q}_\tau + \hat{V}^T \bar{Q}_\tau \hat{A} + \hat{V}^T C^T \hat{C} - \hat{V}^T C_\tau^T \hat{C}_\tau = 0.$$

Since $\hat{V}^T \hat{W} = I$ and $C_\tau \hat{V} = \hat{C}_\tau$,

$$\hat{A}^T + \hat{A} + \hat{C}^T \hat{C} - \hat{C}_\tau^T \hat{C}_\tau = 0.$$

Due to uniqueness, $\hat{Q}_\tau = I$ and thus $\bar{Q}_\tau^T B - \hat{Q}_\tau B = 0$. This completes the proof. \square

$\hat{V}\hat{B}_\tau$ and $\hat{C}_\tau\hat{W}^T$ are projection-based approximations of B_τ and C_τ , respectively. Thus $B_\tau \neq \hat{V}\hat{B}_\tau$ and $C_\tau \neq \hat{C}_\tau\hat{W}^T$, in general. The Krylov-subspace based methods to obtain approximations of B_τ and C_τ as $\hat{V}\hat{B}_\tau$ and $\hat{C}_\tau\hat{W}^T$, respectively, can be found in (Kürschner, 2018).

4.3. Equivalence between the optimality conditions

In (Zulfqar et al., 2019), it is shown that the interpolation conditions (18) and (19) are equivalent to (26) and (27), respectively, when $G(s)$ and $\hat{G}(s)$ have simple poles. In this subsection, we establish equivalence between (some of) the gramians-based optimality conditions in (Goyal and Redmann, 2019) and the interpolation-based optimality conditions in (Sinani and Gugercin, 2019) for the $\mathcal{H}_{2,\tau}$ -optimal MOR problem when $G(s)$ and $\hat{G}(s)$ have simple poles. Further, the interpolation conditions in (Sinani and Gugercin, 2019) and Zulfqar et al. (2020b) are shown to be equivalent when $G(s)$ and $\hat{G}(s)$ have simple poles.

Theorem 4.4. *When $G(s)$ and $\hat{G}(s)$ have simple poles, the following statements are true:*

- (1) *The optimality condition (22) is equivalent to the tangential interpolation condition (31).*
- (2) *The tangential interpolation conditions (31) and (25) are equivalent.*
- (3) *The optimality condition (21) is equivalent to the tangential interpolation condition (30).*
- (4) *The tangential interpolation conditions (30) and (24) are equivalent.*

Proof. (1) Let us define $\bar{\mathcal{P}}_\tau$ as $\bar{\mathcal{P}}_\tau = \bar{P}_\tau \hat{R}^{-T}$. By noting that $e^{\hat{A}\tau} = \hat{R}e^{\hat{\Lambda}\tau}\hat{R}^{-1}$ and multiplying \hat{R}^{-T} from the right, the equation (10) becomes

$$A\bar{\mathcal{P}}_\tau + \bar{\mathcal{P}}_\tau \hat{\Lambda} + B\bar{B}^T - B_\tau \bar{B}^T e^{\hat{A}\tau} = 0.$$

Since $\hat{\Lambda}$ (and resultantly $e^{\hat{A}\tau}$) is a diagonal matrix (Goyal and Redmann, 2019), $\bar{\mathcal{P}}_\tau$ can be computed column-wise as

$$\bar{\mathcal{P}}_{\tau,i} = (-\hat{\lambda}_i I - A)^{-1} B \hat{r}_i - (-\hat{\lambda}_i I - A)^{-1} B_\tau e^{\hat{\lambda}_i \tau} \hat{r}_i.$$

Further, let us define $\hat{\mathcal{P}}_\tau$ as $\hat{\mathcal{P}}_\tau = \hat{P}_\tau \hat{R}^{-T}$. By multiplying \hat{R}^{-T} from the right, the equation (12) becomes

$$\hat{A}\hat{\mathcal{P}}_\tau + \hat{\mathcal{P}}_\tau \hat{\Lambda} + \hat{B}\bar{B}^T - \hat{B}_\tau \bar{B}^T e^{\hat{A}\tau} = 0.$$

Then $\hat{\mathcal{P}}_\tau$ can be computed column-wise as

$$\hat{\mathcal{P}}_{\tau,i} = (-\hat{\lambda}_i I - \hat{A})^{-1} \hat{B} \hat{r}_i - (-\hat{\lambda}_i I - \hat{A})^{-1} \hat{B}_\tau e^{\hat{\lambda}_i \tau} \hat{r}_i.$$

Now, the optimality condition (22) can be written as

$$C [\bar{\mathcal{P}}_{\tau,1} \ \cdots \ \bar{\mathcal{P}}_{\tau,r}] \hat{R}^T - \hat{C} [\hat{\mathcal{P}}_{\tau,1} \ \cdots \ \hat{\mathcal{P}}_{\tau,r}] \hat{R}^T = 0. \quad (39)$$

After multiplying \hat{R}^{-T} from the right, each column of (39) becomes

$$G_{\mathcal{T}}(-\hat{\lambda}_i)\tilde{r}_i - \hat{G}_{\mathcal{T}}(-\hat{\lambda}_i)\tilde{r}_i = 0.$$

- (2) Note that $B_{\tau} = R e^{\Lambda\tau} R^{-1} B$ and $\hat{B}_{\tau} = \hat{R} e^{\hat{\Lambda}\tau} \hat{R}^{-1} \hat{B}$. Thus $G_{\mathcal{T}}(s)$ and $\hat{G}_{\mathcal{T}}(s)$ can be represented as

$$\begin{aligned} G_{\mathcal{T}}(s) &= \left[\sum_{i=1}^n \frac{l_i r_i^T}{s - \lambda_i} \quad - \sum_{i=1}^n \frac{l_i r_i^T}{s - \lambda_i} e^{\lambda_i \tau} \right] = [G(s) \quad e^{s\tau} G_{\tau}(s)], \\ \hat{G}_{\mathcal{T}}(s) &= \left[\sum_{i=1}^r \frac{\hat{l}_i \hat{r}_i^T}{s - \hat{\lambda}_i} \quad - \sum_{i=1}^r \frac{\hat{l}_i \hat{r}_i^T}{s - \hat{\lambda}_i} e^{\hat{\lambda}_i \tau} \right] = [\hat{G}(s) \quad e^{s\tau} \hat{G}_{\tau}(s)]. \end{aligned}$$

Then it can readily be noted that $G_{\mathcal{T}}(-\hat{\lambda}_i)\tilde{r}_i = T_{\tau}(-\hat{\lambda}_i)\hat{r}_i$ and $\hat{G}_{\mathcal{T}}(-\hat{\lambda}_i)\tilde{r}_i = \hat{T}_{\tau}(-\hat{\lambda}_i)\hat{r}_i$.

- (3) Let us define $\bar{\mathcal{Q}}_{\tau}$ as $\bar{\mathcal{Q}}_{\tau} = \bar{Q}_{\tau} \hat{R}$. By multiplying \hat{R} from the right, the equation (11) becomes

$$A^T \bar{\mathcal{Q}}_{\tau} + \bar{\mathcal{Q}}_{\tau} \hat{\Lambda} + C^T \tilde{C} - C_{\tau}^T \tilde{C} e^{\hat{\Lambda}\tau} = 0.$$

Then $\bar{\mathcal{Q}}_{\tau}$ can be computed column-wise as

$$\bar{\mathcal{Q}}_{\tau,i} = (-\hat{\lambda}_i I - A^T)^{-1} C^T \hat{l}_i - (-\hat{\lambda}_i I - A^T)^{-1} C_{\tau}^T e^{\hat{\lambda}_i \tau} \hat{l}_i.$$

Now define $\hat{\mathcal{Q}}_{\tau}$ as $\hat{\mathcal{Q}}_{\tau} = \hat{Q}_{\tau} \hat{R}$. By multiplying \hat{R} from the right, the equation (13) becomes

$$\hat{A}^T \hat{\mathcal{Q}}_{\tau} + \hat{\mathcal{Q}}_{\tau} \hat{\Lambda} + \hat{C}^T \tilde{C} - \hat{C}_{\tau}^T \tilde{C} e^{\hat{\Lambda}\tau} = 0.$$

Then $\hat{\mathcal{Q}}_{\tau}$ can be computed column-wise as

$$\hat{\mathcal{Q}}_{\tau,i} = (-\hat{\lambda}_i I - \hat{A}^T)^{-1} \hat{C}^T \hat{l}_i - (-\hat{\lambda}_i I - \hat{A}^T)^{-1} \hat{C}_{\tau}^T e^{\hat{\lambda}_i \tau} \hat{l}_i.$$

Further, the optimality condition (21) can be written as

$$B^T [\bar{\mathcal{Q}}_{\tau,1} \ \cdots \ \bar{\mathcal{Q}}_{\tau,r}] \hat{R} - \hat{B}^T [\hat{\mathcal{Q}}_{\tau,1} \ \cdots \ \hat{\mathcal{Q}}_{\tau,r}] \hat{R} = 0. \quad (40)$$

After multiplying \hat{R}^{-1} from the right, each column of (40) becomes

$$H_{\mathcal{T}}^T(-\hat{\lambda}_i)\tilde{l}_i - \hat{H}_{\mathcal{T}}^T(-\hat{\lambda}_i)\tilde{l}_i = 0.$$

- (4) Note that $C_{\tau} = C R e^{\Lambda\tau} R^{-1}$ and $\hat{C}_{\tau} = \hat{C} \hat{R} e^{\hat{\Lambda}\tau} \hat{R}^{-1}$. Thus $H_{\mathcal{T}}(s)$ and $\hat{H}_{\mathcal{T}}(s)$ can

be represented as

$$H_{\mathcal{T}}(s) = \begin{bmatrix} \sum_{i=1}^n \frac{l_i r_i^T}{s - \lambda_i} \\ \sum_{i=1}^n \frac{l_i r_i^T}{s - \lambda_i} e^{\lambda_i \tau} \end{bmatrix} = \begin{bmatrix} G(s) \\ e^{s\tau} G_{\tau}(s) \end{bmatrix},$$

$$\hat{H}_{\mathcal{T}}(s) = \begin{bmatrix} \sum_{i=1}^r \frac{\hat{l}_i \hat{r}_i^T}{s - \hat{\lambda}_i} \\ \sum_{i=1}^r \frac{\hat{l}_i \hat{r}_i^T}{s - \hat{\lambda}_i} e^{\hat{\lambda}_i \tau} \end{bmatrix} = \begin{bmatrix} \hat{G}(s) \\ e^{s\tau} \hat{G}_{\tau}(s) \end{bmatrix}.$$

Then it can readily be noted that $\tilde{l}_i^T H_{\mathcal{T}}(-\hat{\lambda}_i) = \tilde{l}_i^T T_{\tau}(-\hat{\lambda}_i)$ and $\tilde{l}_i^T \hat{H}_{\mathcal{T}}(-\hat{\lambda}_i) = \hat{\tilde{l}}_i^T \hat{T}_{\tau}(-\hat{\lambda}_i)$. □

5. $\mathcal{H}_{2,\omega}$ - and $\mathcal{H}_{2,\tau}$ near-optimal MOR

Owing to the difficulty in achieving a local optimum within the oblique projection framework, we focus on achieving near-optimal ROMs for the $\mathcal{H}_{2,\omega}$ - and $\mathcal{H}_{2,\tau}$ -optimal MOR problems. To that end, we propose two frameworks: interpolation-based framework and stationary point iteration framework. The interpolation-based framework does not satisfy any optimality condition exactly, in general. However, deviations in satisfaction of the optimality conditions decay as the order of ROM grows. The stationary point iteration framework, on the other hand, satisfies two out of three optimality conditions upon convergence, and deviation in satisfaction of the third optimality condition decays as the order of ROM grows.

5.1. Interpolation framework

The interpolation theory has been significantly advanced in the last two decades (Astolfi et al., 2020; Grimme, 1997). There are several computational efficient numerical methods to enforce interpolation conditions (Beattie and Gugercin, 2017), which has motivated the results of this subsection. We propose iterative tangential interpolation algorithms that target a subset of respective optimality conditions for the $\mathcal{H}_{2,\omega}$ - and $\mathcal{H}_{2,\tau}$ -optimal MOR problems. The proposed algorithms nearly satisfy their respective optimality conditions upon convergence, and as the order of ROM grows, deviations in satisfaction of the optimality conditions decay further.

We have already seen that the following tangential interpolation conditions are equivalent

$$\begin{aligned} \tilde{l}_i^T T_{\omega}(-\hat{\lambda}_i) = \tilde{l}_i^T \hat{T}_{\omega}(-\hat{\lambda}_i) & \iff \tilde{l}_i^T H_{\Omega}(-\hat{\lambda}_i) = \tilde{l}_i^T \hat{H}_{\Omega}(-\hat{\lambda}_i), \\ T_{\omega}(-\hat{\lambda}_i) \hat{r}_i = \hat{T}_{\omega}(-\hat{\lambda}_i) \hat{r}_i & \iff G_{\Omega}(-\hat{\lambda}_i) \bar{r}_i = \hat{G}_{\Omega}(-\hat{\lambda}_i) \bar{r}_i \end{aligned}$$

when $G(s)$ and $\hat{G}(s)$ have simple poles. To satisfy these conditions, we need an interpolation framework that preserves the structure of (state-space realizations of) $H_{\Omega}(s)$ and $G_{\Omega}(s)$ in $\hat{H}_{\Omega}(s)$ and $\hat{G}_{\Omega}(s)$, respectively. The triplet $(-\hat{\lambda}_i, \hat{r}_i, \hat{l}_i)$ is not known a priori, and thus finding such a ROM is a nonconvex problem. We propose an iterative algorithm, wherein starting with an arbitrary guess, the triplet $(-\hat{\lambda}_i, \hat{r}_i, \hat{l}_i)$ is updated in each iteration until convergence. The proposed algorithm is referred to as the ‘‘Frequency-limited iterative tangential interpolation algorithm (FLITIA)’. The

pseudo-code of FLITIA is given in Algorithm 1. Steps 1-4 are standard interpolation results (already discussed in Subsection 3.1). Steps 5-9 are the bi-orthogonal Gram-Schmidt method to ensure the oblique projection condition $\hat{W}^T \hat{V} = I$; cf. Benner et al. (2011). The ROM $\hat{G}(s)$ is fetched from the ROMs of $G_\Omega(s)$ and $H_\Omega(s)$ in Step 10. The interpolation data is updated in Steps 11-13. In general, \tilde{B}_Ω and \tilde{C}_Ω are not equal to \hat{B}_Ω and \hat{C}_Ω , respectively, because $\hat{W}^T F_\omega[A]B \neq F_\omega[\hat{A}]B$ and $C F_\omega[A]\hat{V} \neq C F_\omega[\hat{A}]$. However, as the order of ROM grows, $\hat{V} F_\omega[\hat{A}]\hat{W}^T \approx F_\omega[A]$ because $\hat{V} F_\omega[\hat{A}]\hat{W}^T$ is the oblique projection-based approximation of $F_\omega[A]$. Thus \tilde{B}_Ω and \tilde{C}_Ω become nearly equal to \hat{B}_Ω and \hat{C}_Ω , respectively. Finally, upon convergence, the interpolation conditions (26) and (27) are nearly satisfied.

Algorithm 1 FLITIA

Input: Original system: (A, B, C) ; Desired frequency interval: $[-\omega, \omega]$ rad/sec; Initial guess: $(\hat{\sigma}_i, \hat{b}_i, \hat{c}_i)$.

Output: ROM $(\hat{A}, \hat{B}, \hat{C})$.

- 1: Set $B_\Omega = [B \quad F_\omega[A]B]$ and $C_\Omega = \begin{bmatrix} C \\ C F_\omega[A] \end{bmatrix}$.
 - 2: **while** (not converged) **do**
 - 3: $\bar{b}_i = \begin{bmatrix} F_\omega[-\hat{\sigma}_i]\hat{b}_i \\ \hat{b}_i \end{bmatrix}$ and $\bar{c}_i = [F_\omega[-\hat{\sigma}_i]\hat{c}_i \quad \hat{c}_i]$.
 - 4: Compute \hat{V} and \hat{W} from the equations (28) and (29), respectively.
 - 5: **for** $i = 1, \dots, r$ **do**
 - 6: $\hat{v} = \hat{V}(:, i)$, $\hat{v} = \prod_{k=1}^i (I - \hat{V}(:, k)\hat{W}(:, k)^T)\hat{v}$.
 - 7: $\hat{w} = \hat{W}(:, i)$, $\hat{w} = \prod_{k=1}^i (I - \hat{W}(:, k)\hat{V}(:, k)^T)\hat{w}$.
 - 8: $\hat{v} = \frac{\hat{v}}{\|\hat{v}\|_2}$, $\hat{w} = \frac{\hat{w}}{\|\hat{w}\|_2}$, $\hat{v} = \frac{\hat{v}}{\hat{w}^T \hat{v}}$, $\hat{V}(:, i) = \hat{v}$, $\hat{W}(:, i) = \hat{w}$.
 - 9: **end for**
 - 10: $\hat{A} = \hat{W}^T A \hat{V}$, $\tilde{B}_\Omega = \hat{W}^T B_\Omega = [\hat{B} \quad \hat{W}^T F_\omega[A]B]$, $\tilde{C}_\Omega = C_\Omega \hat{V} = \begin{bmatrix} \hat{C} \\ C F_\omega[A]\hat{V} \end{bmatrix}$.
 - 11: Compute spectral factorization of $\hat{A} = \hat{R}\hat{\Lambda}\hat{R}^{-1}$ where $\hat{\Lambda} = \text{diag}(\hat{\lambda}_1, \dots, \hat{\lambda}_r)$.
 - 12: Set $[\hat{r}_1 \quad \dots \quad \hat{r}_r] = \hat{B}^T \hat{R}^{-*}$ and $[\hat{l}_1 \quad \dots \quad \hat{l}_r] = \hat{C} \hat{R}$.
 - 13: Update $\hat{\sigma}_i = -\hat{\lambda}_i$, $\hat{b}_i = \hat{r}_i$, and $\hat{c}_i^T = \hat{l}_i$.
 - 14: **end while**
-

Similarly, we have seen that the following tangential interpolation conditions are equivalent

$$\begin{aligned} \tilde{l}_i^T T_\tau(-\hat{\lambda}_i) &= \tilde{l}_i^T \hat{T}_\tau(-\hat{\lambda}_i) && \iff && \tilde{l}_i^T H_\mathcal{T}(-\hat{\lambda}_i) &= \tilde{l}_i^T \hat{H}_\mathcal{T}(-\hat{\lambda}_i), \\ T_\tau(-\hat{\lambda}_i)\hat{r}_i &= \hat{T}_\tau(-\hat{\lambda}_i)\hat{r}_i && \iff && G_\mathcal{T}(-\hat{\lambda}_i)\tilde{r}_i &= \hat{G}_\mathcal{T}(-\hat{\lambda}_i)\tilde{r}_i. \end{aligned}$$

when $G(s)$ and $\hat{G}(s)$ have simple poles. To satisfy these conditions, we need an interpolation framework that preserves the structure of (state-space realizations of) $H_\mathcal{T}(s)$ and $G_\mathcal{T}(s)$ in $\hat{H}_\mathcal{T}(s)$ and $\hat{G}_\mathcal{T}(s)$, respectively. We propose an iterative algorithm, wherein starting with an arbitrary guess, the triplet $(-\hat{\lambda}_i, \hat{r}_i, \hat{l}_i)$ is updated in each iteration until convergence. The proposed algorithm is referred to as the ‘‘Time-limited iterative tangential interpolation algorithm (TLITIA)’. The pseudo-code of TLITIA is given in Algorithm 2. Steps 1-4 are standard interpolation results (already discussed in Subsection 3.4). Steps 5-9 are the bi-orthogonal Gram-Schmidt method to ensure the oblique

projection condition $\hat{W}^T \hat{V} = I$. The ROM $\hat{G}(s)$ is fetched from the ROMs of $G_{\mathcal{T}}(s)$ and $H_{\mathcal{T}}(s)$ in Step 10. The interpolation data is updated in Steps 11-13. In general, $\tilde{B}_{\mathcal{T}}$ and $\tilde{C}_{\mathcal{T}}$ are not equal to $\hat{B}_{\mathcal{T}}$ and $\hat{C}_{\mathcal{T}}$, respectively, because $\hat{W}^T e^{A\tau} B \neq e^{\hat{A}\tau} \hat{B}$ and $C e^{A\tau} \hat{V} \neq \hat{C} e^{\hat{A}\tau}$. Thus the structures of $B_{\mathcal{T}}$ and $C_{\mathcal{T}}$ are not preserved in $\hat{W}^T B_{\mathcal{T}}$ and $C_{\mathcal{T}} \hat{V}$, respectively. However, as the order of ROM grows, $\hat{V} e^{\hat{A}t} \hat{W}^T \approx e^{At}$ because $\hat{V} e^{\hat{A}t} \hat{W}^T$ is the oblique projection-based approximation of e^{At} . Thus $\tilde{B}_{\mathcal{T}}$ and $\tilde{C}_{\mathcal{T}}$ become nearly equal to $\hat{B}_{\mathcal{T}}$ and $\hat{C}_{\mathcal{T}}$, respectively. Finally, upon convergence, the interpolation conditions (30) and (31) are nearly satisfied.

Algorithm 2 TLITIA

Input: Original system: (A, B, C) ; Desired time interval: $[0, \tau]$ sec; Initial guess: $(\hat{\sigma}_i, \hat{b}_i, \hat{c}_i)$.

Output: ROM $(\hat{A}, \hat{B}, \hat{C})$.

- 1: Set $B_{\mathcal{T}} = [B \quad -e^{A\tau} B]$ and $C_{\mathcal{T}} = \begin{bmatrix} C \\ -C e^{A\tau} \end{bmatrix}$.
 - 2: **while** (not converged) **do**
 - 3: $\bar{b}_i = \begin{bmatrix} \hat{b}_i \\ e^{-\sigma_i \tau} \hat{b}_i \end{bmatrix}$ and $\bar{c}_i = [\hat{c}_i \quad e^{-\sigma_i \tau} \hat{c}_i]$.
 - 4: Compute \hat{V} and \hat{W} from the equations (32) and (33), respectively.
 - 5: **for** $i = 1, \dots, r$ **do**
 - 6: $\hat{v} = \hat{V}(:, i)$, $\hat{v} = \prod_{k=1}^i (I - \hat{V}(:, k) \hat{W}(:, k)^T) \hat{v}$.
 - 7: $\hat{w} = \hat{W}(:, i)$, $\hat{w} = \prod_{k=1}^i (I - \hat{W}(:, k) \hat{V}(:, k)^T) \hat{w}$.
 - 8: $\hat{v} = \frac{\hat{v}}{\|\hat{v}\|_2}$, $\hat{w} = \frac{\hat{w}}{\|\hat{w}\|_2}$, $\hat{v} = \frac{\hat{v}}{\hat{w}^T \hat{v}}$, $\hat{V}(:, i) = \hat{v}$, $\hat{W}(:, i) = \hat{w}$.
 - 9: **end for**
 - 10: $\hat{A} = \hat{W}^T A \hat{V}$, $\tilde{B}_{\mathcal{T}} = \hat{W}^T B_{\mathcal{T}} = [\hat{B} \quad -\hat{W}^T e^{A\tau} B]$, $\tilde{C}_{\mathcal{T}} = C_{\mathcal{T}} \hat{V} = \begin{bmatrix} \hat{C} \\ -C e^{A\tau} \hat{V} \end{bmatrix}$.
 - 11: Compute spectral factorization of $\hat{A} = \hat{R} \hat{\Lambda} \hat{R}^{-1}$ where $\hat{\Lambda} = \text{diag}(\hat{\lambda}_1, \dots, \hat{\lambda}_r)$.
 - 12: Set $[\hat{r}_1 \quad \dots \quad \hat{r}_r] = \hat{B}^T \hat{R}^{-*}$ and $[\hat{l}_1 \quad \dots \quad \hat{l}_r] = \hat{C} \hat{R}$.
 - 13: Update $\hat{\sigma}_i = -\hat{\lambda}_i$, $\hat{b}_i = \hat{r}_i$, and $\hat{c}_i^T = \hat{l}_i$.
 - 14: **end while**
-

5.2. Stationary point iteration framework

Owing to the inherent difficulty in making an optimal choice of \hat{A} within the oblique projection framework, we now focus on constructing a ROM $(\hat{A}, \hat{B}, \hat{C})$ wherein \hat{B} and C are the optimal choices. Let the ROM be obtained by using the oblique projection $\Pi = \bar{P}_{\omega} \hat{P}_{\omega}^{-1} \hat{Q}_{\omega}^{-1} \bar{Q}_{\omega}^T$ (with $\hat{V} = \bar{P}_{\omega} \hat{P}_{\omega}^{-1}$ and $\hat{W} = \bar{Q}_{\omega} \hat{Q}_{\omega}^{-1}$). Since \bar{P}_{ω} , \hat{P}_{ω} , \bar{Q}_{ω} , and \hat{Q}_{ω} depend on the ROM $(\hat{A}, \hat{B}, \hat{C})$, finding such a projection is a nonconvex problem. Note that (1) and the equations (4)-(7) can be seen as the following coupled system of equations

$$(\hat{A}, \hat{B}, \hat{C}) = f_{\omega}(\bar{P}_{\omega}, \hat{P}_{\omega}, \bar{Q}_{\omega}, \hat{Q}_{\omega}), \quad (\bar{P}_{\omega}, \hat{P}_{\omega}, \bar{Q}_{\omega}, \hat{Q}_{\omega}) = g_{\omega}(\hat{A}, \hat{B}, \hat{C}).$$

The stationary points of $(\hat{A}, \hat{B}, \hat{C}) = f_{\omega}(g_{\omega}(\hat{A}, \hat{B}, \hat{C}))$ satisfy the optimality conditions (15) and (16). The pseudo-code of the stationary point iteration algorithm to compute stationary points of $(\hat{A}, \hat{B}, \hat{C}) = f_{\omega}(g_{\omega}(\hat{A}, \hat{B}, \hat{C}))$ is given in Algorithm 3, which is

referred to as the “Frequency-limited \mathcal{H}_2 -suboptimal MOR (FLHMOR)”. The oblique projection condition $\hat{W}^T \hat{V} = I$ is ensured by using the biorthogonal Gram-Schmidt method, i.e., steps 5-9.

Algorithm 3 FLHMOR

Input: Original system: (A, B, C) ; Desired frequency interval: $[-\omega, \omega]$ rad/sec; Initial guess: $(\hat{A}, \hat{B}, \hat{C})$.

Output: ROM $(\hat{A}, \hat{B}, \hat{C})$.

- 1: **while** (not converged) **do**
 - 2: Solve the equations (4) and (5) to compute \bar{P}_ω and \bar{Q}_ω , respectively.
 - 3: Solve the equations (6) and (7) to compute \hat{P}_ω and \hat{Q}_ω , respectively.
 - 4: Set $\hat{V} = \bar{P}_\omega \hat{P}_\omega^{-1}$ and $\hat{W} = \bar{Q}_\omega \hat{Q}_\omega^{-1}$.
 - 5: **for** $i = 1, \dots, r$ **do**
 - 6: $\hat{v} = \hat{V}(:, i)$, $\hat{v} = \prod_{k=1}^i (I - \hat{V}(:, k) \hat{W}(:, k)^T) \hat{v}$.
 - 7: $\hat{w} = \hat{W}(:, i)$, $\hat{w} = \prod_{k=1}^i (I - \hat{W}(:, k) \hat{V}(:, k)^T) \hat{w}$.
 - 8: $\hat{v} = \frac{\hat{v}}{\|\hat{v}\|_2}$, $\hat{w} = \frac{\hat{w}}{\|\hat{w}\|_2}$, $\hat{v} = \frac{\hat{v}}{\hat{w}^T \hat{v}}$, $\hat{V}(:, i) = \hat{v}$, $\hat{W}(:, i) = \hat{w}$.
 - 9: **end for**
 - 10: $\hat{A} = \hat{W}^T A \hat{V}$, $\hat{B} = \hat{W}^T B$, $\hat{C} = C \hat{V}$.
 - 11: **end while**
-

Similarly, if the ROM is obtained by using the oblique projections $\Pi = \bar{P}_\tau \hat{P}_\tau^{-1} \hat{Q}_\tau^{-1} \bar{Q}_\tau^T$ (with $\hat{V} = \bar{P}_\tau \hat{P}_\tau^{-1}$ and $\hat{W} = \bar{Q}_\tau \hat{Q}_\tau^{-1}$), (1) and the equations (10)-(13) can be seen as the following coupled system of equations

$$(\hat{A}, \hat{B}, \hat{C}) = f_\tau(\bar{P}_\tau, \hat{P}_\tau, \bar{Q}_\tau, \hat{Q}_\tau), \quad (\bar{P}_\tau, \hat{P}_\tau, \bar{Q}_\tau, \hat{Q}_\tau) = g_\tau(\hat{A}, \hat{B}, \hat{C}).$$

The stationary points of $(\hat{A}, \hat{B}, \hat{C}) = f_\tau(g_\tau(\hat{A}, \hat{B}, \hat{C}))$ satisfy the optimality conditions (21) and (22). The pseudo-code of the stationary point iteration algorithm to compute stationary points of $(\hat{A}, \hat{B}, \hat{C}) = f_\tau(g_\tau(\hat{A}, \hat{B}, \hat{C}))$ is given in Algorithm 4, which is referred to as the “Time-limited \mathcal{H}_2 -suboptimal MOR (TLHMOR)”. The oblique projection condition $\hat{W}^T \hat{V} = I$ is again ensured by using the biorthogonal Gram-Schmidt method.

6. Computational aspects

In this section, we briefly discuss some important computational aspects to be considered for efficient implementation of the proposed algorithms.

Generic frequency and time intervals: Throughout the paper, the desired frequency and time intervals are assumed for simplicity to be $\Omega = [-\omega, \omega]$ rad/sec and $\mathcal{T} = [0, \tau]$ sec, respectively. With some modifications, the proposed algorithms can be generalized for any generic frequency and time interval, i.e., $\Omega = [-\omega_2, -\omega_1] \cup [\omega_1, \omega_2]$ rad/sec and $\mathcal{T} = [\tau_1, \tau_2]$ sec, respectively. For the generic case, $F_\omega[A]$ and $F_\omega[-\hat{\sigma}_i]$ in FLITIA and FLHMOR are computed as the following

$$F_\omega[A] = F_{\omega_2}[A] - F_{\omega_1}[A] \quad \text{and} \quad F_\omega[A] = F_{\omega_2}[-\hat{\sigma}_i] - F_{\omega_1}[-\hat{\sigma}_i].$$

Algorithm 4 TLHMOR

Input: Original system: (A, B, C) ; Desired time interval: $[0, \tau]$ sec; Initial guess: $(\hat{A}, \hat{B}, \hat{C})$.

Output: ROM $(\hat{A}, \hat{B}, \hat{C})$.

- 1: **while** (not converged) **do**
 - 2: Solve the equations (10) and (11) to compute \bar{P}_τ and \bar{Q}_τ , respectively.
 - 3: Solve the equations (12) and (13) to compute \hat{P}_τ and \hat{Q}_τ , respectively.
 - 4: Set $\hat{V} = \bar{P}_\tau \hat{P}_\tau^{-1}$ and $\hat{W} = \bar{Q}_\tau \hat{Q}_\tau^{-1}$.
 - 5: **for** $i = 1, \dots, r$ **do**
 - 6: $\hat{v} = \hat{V}(:, i)$, $\hat{v} = \prod_{k=1}^i (I - \hat{V}(:, k) \hat{W}(:, k)^T) \hat{v}$.
 - 7: $\hat{w} = \hat{W}(:, i)$, $\hat{w} = \prod_{k=1}^i (I - \hat{W}(:, k) \hat{V}(:, k)^T) \hat{w}$.
 - 8: $\hat{v} = \frac{\hat{v}}{\|\hat{v}\|_2}$, $\hat{w} = \frac{\hat{w}}{\|\hat{w}\|_2}$, $\hat{v} = \frac{\hat{v}}{\hat{w}^T \hat{v}}$, $\hat{V}(:, i) = \hat{v}$, $\hat{W}(:, i) = \hat{w}$.
 - 9: **end for**
 - 10: $\hat{A} = \hat{W}^T A \hat{V}$, $\hat{B} = \hat{W}^T B$, $\hat{C} = C \hat{V}$.
 - 11: **end while**
-

For the generic case, $B_{\mathcal{T}}$, $C_{\mathcal{T}}$, \bar{b}_i , and \bar{c}_i in TLITIA are computed as

$$B_{\mathcal{T}} = \begin{bmatrix} e^{At_1} B & -e^{At_2} B \end{bmatrix}, \quad C_{\mathcal{T}} = \begin{bmatrix} C e^{At_1} \\ -C e^{At_2} \end{bmatrix},$$
$$\bar{b}_i = \begin{bmatrix} e^{-\sigma_i t_1} \hat{b}_i \\ e^{-\sigma_i t_2} \hat{b}_i \end{bmatrix}, \quad \bar{c}_i = \begin{bmatrix} e^{-\sigma_i t_1} \hat{c}_i & e^{-\sigma_i t_2} \hat{c}_i \end{bmatrix}.$$

On similar lines, for the generic case, \bar{P}_τ , \hat{P}_τ , \bar{Q}_τ , and \hat{Q}_τ in TLHMOR are computed as the following

$$\begin{aligned} A \bar{P}_\tau + \bar{P}_\tau \hat{A}^T + e^{At_1} B \hat{B}^T e^{\hat{A}^T t_1} - e^{At_2} B \hat{B}^T e^{\hat{A}^T t_2} &= 0, \\ \hat{A} \hat{P}_\tau + \hat{P}_\tau \hat{A}^T + e^{\hat{A} t_1} \hat{B} \hat{B}^T e^{\hat{A}^T t_1} - e^{\hat{A} t_2} \hat{B} \hat{B}^T e^{\hat{A}^T t_2} &= 0, \\ A^T \bar{Q}_\tau + \bar{Q}_\tau \hat{A} + e^{A^T t_1} C^T \hat{C} e^{\hat{A} t_1} - e^{A^T t_2} C^T \hat{C} e^{\hat{A} t_2} &= 0, \\ \hat{A}^T \hat{Q}_\tau + \hat{Q}_\tau \hat{A} + e^{\hat{A}^T t_1} \hat{C}^T \hat{C} e^{\hat{A} t_1} - e^{\hat{A}^T t_2} \hat{C}^T \hat{C} e^{\hat{A} t_2} &= 0. \end{aligned}$$

Computation of $F_\omega[A]$ and $e^{A\tau}$: As the order of the original model becomes high, the computation of $F_\omega[A]$ and $e^{A\tau}$ becomes expensive. In this scenario, $F_\omega[A]$ and $e^{A\tau}$ can be approximated as $\hat{V} F_\omega[\hat{A}] \hat{W}^T$ and $\hat{V} e^{\hat{A}\tau} \hat{W}^T$, respectively. The Krylov subspace-based methods to compute \hat{V} and \hat{W} for this purpose can be found in (Benner et al., 2016; Kürschner, 2018).

Computation of \bar{P}_ω , \bar{Q}_ω , \bar{P}_τ , and \bar{Q}_τ : In general, $p \ll n$, $m \ll n$, and the matrices A , B , and C are sparse in a large-scale setting. This makes the equations (4), (5), (10), and (11) a special type of Sylvester equation known as “*sparse-dense*” Sylvester equation in the literature, cf. (Benner et al., 2011), wherein the large-scale matrices are small, and the small-scale matrices are dense. An efficient solver for this class of Sylvester equation that can be used to compute \bar{P}_ω , \bar{Q}_ω , \bar{P}_τ , and \bar{Q}_τ efficiently in a large-scale setting is proposed in (Benner et al., 2011).

Approximations of P_ω , Q_ω , P_τ , Q_τ : If either the condition (15) or (16) is met, the

following holds

$$\|E(s)\|_{\mathcal{H}_{2,\omega}}^2 = \text{tr}(C(\bar{P}_\omega - \hat{V}\hat{P}_\omega\hat{V}^T)C^T) = \text{tr}(B^T(\bar{Q}_\omega - \hat{W}\hat{Q}_\omega\hat{W}^T)B).$$

Thus, it can readily be concluded that FLITIA and FLHMOR provide approximations of P_ω and Q_ω as $\tilde{P}_\omega = \hat{V}\hat{P}_\omega\hat{V}^T$ and $\tilde{Q}_\omega = \hat{W}\hat{Q}_\omega\hat{W}^T$, respectively. \tilde{P}_ω and \tilde{Q}_ω can be used to perform approximate frequency-limited balanced truncation (FLBT) (Gawronski and Juang, 1990) without solving the large-scale Lyapunov equations (2) and (3). Therefore, FLITIA and FLHMOR can be used to reduce the computational cost of FLBT.

Similarly, if either the condition (21) or (22) is met, the following holds

$$\|E(s)\|_{\mathcal{H}_{2,\tau}}^2 = \text{tr}(C(\bar{P}_\tau - \hat{V}\hat{P}_\tau\hat{V}^T)C^T) = \text{tr}(B^T(\bar{Q}_\tau - \hat{W}\hat{Q}_\tau\hat{W}^T)B).$$

Thus, it can readily be concluded that TLITIA and TLHMOR provide approximations of P_τ and Q_τ as $\tilde{P}_\tau = \hat{V}\hat{P}_\tau\hat{V}^T$ and $\tilde{Q}_\tau = \hat{W}\hat{Q}_\tau\hat{W}^T$, respectively. \tilde{P}_τ and \tilde{Q}_τ can be used to perform approximate time-limited balanced truncation (TLBT) (Gawronski and Juang, 1990) without solving the large-scale Lyapunov equations (8) and (9). Therefore, TLITIA and TLHMOR can be used to reduce the computational cost of TLBT.

7. Numerical results

In this section, the proposed algorithms are tested on four test models. The first model is a small-order illustrative system, which is considered to aid convenient validation of the theoretical results presented in the paper. The other three models are high-order systems taken from the collection of benchmark systems for MOR presented in (Chahlaoui and Van Dooren, 2005).

7.1. Experimental setup and hardware

The selection of desired frequency and time intervals is made arbitrarily for demonstration purposes. The initial guess of the ROM in FLHMOR and TLHMOR is also made arbitrarily. The mirror images of the poles and residues of the respective initial guess are used as interpolation points and tangential directions, respectively, in FLITIA and TLITIA. The ROMs are constructed by using FLITIA, TLITIA, FLHMOR, and TLHMOR. The accuracy of the ROMs is compared with that of FLBT and TLBT, as these are considered gold standards of their respective problems. Although FLTSIA and TLIRKA are heuristic in nature and based on experimental results, they are very similar in essence to FLITIA and TLITIA, respectively. Their performance is also quite similar and often indistinguishable. Therefore, we have not shown the results of FLTSIA and TLIRKA in our simulations for clarity. The Lyapunov and Sylvester equations are solved using MATLAB's *lyap* command. The experiments are performed using MATLAB 2016 on a laptop with a 2GHz-i7 Intel processor and 16GB of memory.

7.2. Illustrative example

Consider a sixth-order model with the following state-space realization

$$A = \begin{bmatrix} -1.7682 & 0.4541 & 0.5078 & -0.1395 & -0.1218 & 0.7166 \\ -0.2639 & -2.4685 & -0.6461 & 1.3914 & 0.1109 & 0.3260 \\ 0.1337 & -1.1676 & -2.2543 & 0.0382 & 0.0584 & 0.4749 \\ 0.3569 & 0.2430 & -0.9208 & -2.3415 & 0.2474 & -1.1362 \\ 0.0093 & 0.4753 & 0.1530 & -0.2144 & -2.1098 & 0.1888 \\ 0.8927 & -0.8289 & -0.2549 & -0.6194 & 0.4891 & -2.0675 \end{bmatrix}, \quad B = \begin{bmatrix} 0 & 0 \\ 0.5963 & -0.1135 \\ -0.1556 & 0.8070 \\ 0.1291 & -0.0898 \\ 0 & -0.0301 \\ -0.0301 & -0.0063 \end{bmatrix},$$

$$C = [-0.0919 \quad -0.9212 \quad -0.9270 \quad -0.9612 \quad 1.7848 \quad -0.2002].$$

The initial guess of the ROM used in FLHMOR and TLHMOR is given by

$$\hat{A}^{(0)} = \begin{bmatrix} -0.5763 & -0.5492 \\ -0.6734 & -2.6844 \end{bmatrix}, \quad \hat{B}^{(0)} = \begin{bmatrix} -0.2749 & -1.0346 \\ 0.1071 & 1.6785 \end{bmatrix},$$

$$\hat{C}^{(0)} = [-0.0260 \quad -0.8520].$$

The desired frequency interval in FLHMOR and FLITIA is set to $[-0.5, 0.5]$ rad/sec. The ROM constructed by FLHMOR is given by

$$\hat{A} = \begin{bmatrix} -0.5772 & -0.7972 \\ -0.4698 & -2.6876 \end{bmatrix}, \quad \hat{B} = \begin{bmatrix} 0.1461 & 0.5396 \\ -0.0254 & -0.5516 \end{bmatrix},$$

$$\hat{C} = [0.1027 \quad 2.6474].$$

It can be verified that

$$C\bar{P}_\omega = \hat{C}\hat{P}_\omega = [-0.2169 \quad 0.0679], \quad \bar{Q}_\omega^T B = \hat{Q}_\omega \hat{B} = \begin{bmatrix} 0.0143 & 0.1051 \\ -0.0221 & -0.1778 \end{bmatrix}.$$

However, $\|F_\omega[A] - \hat{V}F_\omega[\hat{A}]\hat{W}^T\|_2 = 0.1502$, which reveals that the optimality condition (14) is not exactly satisfied. The ROM constructed by FLITIA is given by

$$\hat{A} = \begin{bmatrix} -0.6921 & -1.5934 \\ -0.3789 & -2.5727 \end{bmatrix}, \quad \hat{B} = \begin{bmatrix} 0.0931 & 0.7682 \\ -0.0216 & 0.3427 \end{bmatrix},$$

$$\hat{C} = [-0.9933 \quad -1.8726].$$

Interestingly, FLITIA also satisfies the optimality conditions (15) and (16) exactly in this case, and it can be verified that

$$C\bar{P}_\omega = \hat{C}\hat{P}_\omega = [-0.1662 \quad 0.0041], \quad \bar{Q}_\omega^T B = \hat{Q}_\omega \hat{B} = \begin{bmatrix} 0.0275 & 0.2093 \\ -0.0037 & -0.0175 \end{bmatrix}.$$

However, $\|F_\omega[A] - \hat{V}F_\omega[\hat{A}]\hat{W}^T\|_2 = 0.1502$, which reveals that the optimality condition (14) is not exactly satisfied. A closer look at the ROMs constructed by FLHMOR and FLITIA reveals that these are actually different realizations of the same transfer function.

The desired time interval in TLHMOR and TLITIA is set to $[0, 0.1]$ sec. The ROM

constructed by TLHMOR is given by

$$\begin{aligned}\hat{A} &= \begin{bmatrix} -2.5168 & 0.4390 \\ 1.2046 & -2.5553 \end{bmatrix}, & \hat{B} &= \begin{bmatrix} 0.1618 & 0.2539 \\ 0.0342 & 0.6215 \end{bmatrix}, \\ \hat{C} &= [0.68987 \quad -2.5008].\end{aligned}$$

It can be verified that

$$C\bar{P}_\tau = \hat{C}\hat{P}_\tau = [-0.0294 \quad -0.0700], \quad \bar{Q}_\tau^T B = \hat{Q}_\tau \hat{B} = \begin{bmatrix} 0.0003 & -0.0608 \\ -0.0009 & 0.2740 \end{bmatrix}.$$

However, $\|e^{At_2} - \hat{V}e^{\hat{A}t_2}\hat{W}^T\|_2 = 1.4127$, which reveals that the optimality condition (20) is not exactly satisfied. The ROM constructed by TLITIA is given by

$$\begin{aligned}\hat{A} &= \begin{bmatrix} -2.4649 & -1.2215 \\ -0.4291 & -2.6072 \end{bmatrix}, & \hat{B} &= \begin{bmatrix} 0.0020 & -0.5830 \\ 0.1609 & 0.1621 \end{bmatrix}, \\ \hat{C} &= [2.4022 \quad 0.1330].\end{aligned}$$

Interestingly, TLITIA also satisfies the optimality conditions (21) and (22) exactly in this case, and it can be verified that

$$C\bar{P}_\tau = \hat{C}\hat{P}_\tau = [0.0655 \quad -0.0190], \quad \bar{Q}_\tau^T B = \hat{Q}_\tau \hat{B} = \begin{bmatrix} 0.0008 & -0.2655 \\ 0.0001 & 0.0003 \end{bmatrix}.$$

However, $\|e^{At_2} - \hat{V}e^{\hat{A}t_2}\hat{W}^T\|_2 = 1.4127$, which reveals that the optimality condition (20) is not exactly satisfied. A closer look at the ROMs constructed by TLHMOR and TLITIA reveals that these are actually different realizations of the same transfer function.

7.3. Clamped Beam

Let us consider the 348th order clamped beam model as the test system from the benchmark collection of test systems for MOR, cf. (Chahlaoui and Van Dooren, 2005). For the frequency-limited case, the desired frequency interval is chosen as $[-6, -4] \cup [4, 6]$ rad/sec. The clamped beam model is reduced by using FLBT, FLITIA, and FLHMOR, and their accuracy is compared in Table 2. It can be noticed that FLITIA and FLHMOR offer less $\|E(s)\|_{\mathcal{H}_{2,\omega}}$ than FLBT. The frequency-domain error for the

Table 2.: $\|E(s)\|_{\mathcal{H}_{2,\omega}}$

Order	FLBT	FLITIA	FLHMOR
10	0.0118	0.0099	0.0099
11	0.0203	0.0099	0.0099
12	4.2345×10^{-4}	4.1256×10^{-4}	4.1952×10^{-4}
13	2.4317×10^{-4}	2.2695×10^{-4}	2.2364×10^{-4}
14	2.4189×10^{-4}	2.0278×10^{-4}	2.0642×10^{-4}
15	2.4109×10^{-4}	1.9690×10^{-4}	2.0642×10^{-4}

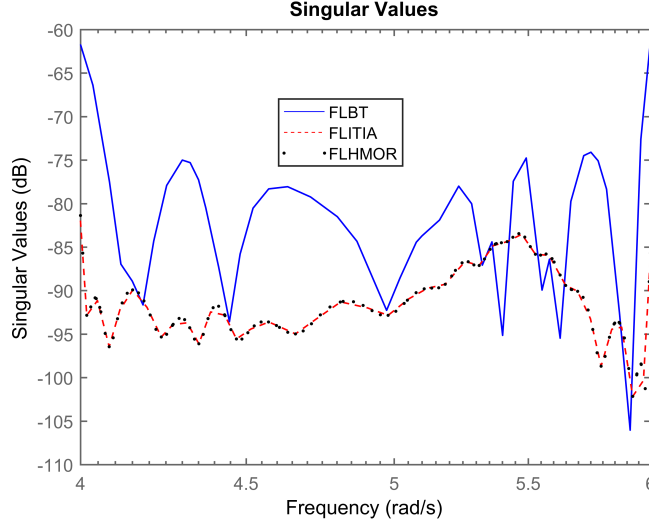


Figure 1.: Singular values of $E(s)$ within $[4, 6]$ rad/sec

ROMs of order 14 within the desired frequency interval is compared in Figure 1. It can be seen that FLITIA and FLHMOR offer better accuracy than FLBT.

For the time-limited case, the desired time interval is chosen as $[0, 1]$ sec. The clamped beam model is reduced by using TLBT, TLITIA, and TLHMOR, and their accuracy is compared in Table 3. It can be noticed that TLITIA and TLHMOR mostly offer less $\|E(s)\|_{\mathcal{H}_{2,\tau}}$ than TLBT. The time-domain error for the ROMs of order 12

Table 3.: $\|E(s)\|_{\mathcal{H}_{2,\tau}}$

Order	TLBT	TLITIA	TLHMOR
10	0.1637	0.1016	0.1016
11	0.1200	0.1051	0.1051
12	0.0872	0.0903	0.0903
13	0.0662	0.0390	0.0390
14	0.0594	0.0586	0.0586
15	0.0018	0.0017	0.0017

within the desired time interval is compared in Figure 2. It can be seen that TLITIA and TLHMOR compare well in accuracy with TLBT.

7.4. Artificial Dynamic System

Let us consider the 1006^{th} order artificial dynamic system model as the test system from the benchmark collection of test systems for MOR, cf. (Chahlaoui and Van Dooren, 2005). For the frequency-limited case, the desired frequency interval is chosen as $[-15, -11] \cup [11, 15]$ rad/sec. The artificial dynamic system model is reduced by using FLBT, FLITIA, and FLHMOR, and their accuracy is compared in Table 4. It can be noticed that FLITIA and FLHMOR mostly offer less $\|E(s)\|_{\mathcal{H}_{2,\omega}}$ than FLBT. The frequency-domain error for the ROMs of order 10 within the desired frequency

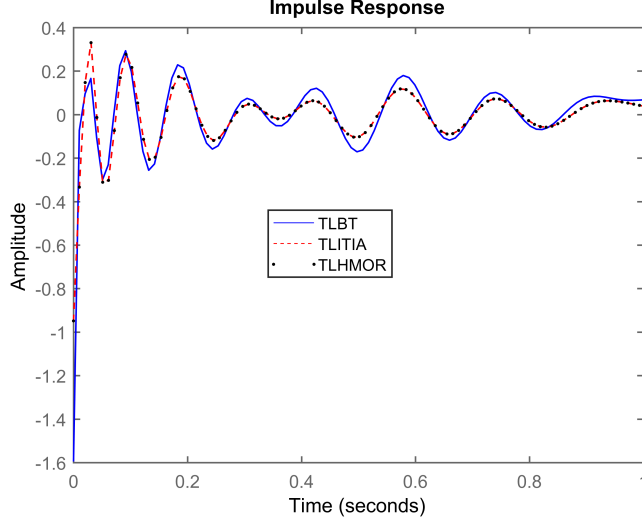


Figure 2.: Impulse response of $E(s)$ within $[0, 1]$ sec

Table 4.: $\|E(s)\|_{\mathcal{H}_{2,\omega}}$

Order	FLBT	FLITIA	FLHMOR
10	2.3514×10^{-5}	3.9357×10^{-6}	2.1685×10^{-5}
11	1.5678×10^{-5}	3.5242×10^{-6}	1.5956×10^{-5}
12	5.7383×10^{-5}	5.8867×10^{-6}	7.2903×10^{-6}
13	4.2452×10^{-5}	2.4202×10^{-5}	6.6805×10^{-6}
14	3.8084×10^{-5}	9.8140×10^{-6}	7.5714×10^{-6}
15	5.8612×10^{-5}	1.7097×10^{-5}	1.6830×10^{-5}

interval is compared in Figure 3. It can be seen that FLITIA and FLHMOR offer better accuracy than FLBT.

For the time-limited case, the desired time interval is chosen as $[0, 2]$ sec. The artificial dynamic system model is reduced by using TLBT, TLITIA, and TLHMOR, and their accuracy is compared in Table 5. It can be noticed that TLITIA and TLHMOR offer less $\|E(s)\|_{\mathcal{H}_{2,\tau}}$ than TLBT. The time-domain error for the ROMs of order 15

Table 5.: $\|E(s)\|_{\mathcal{H}_{2,\tau}}$

Order	TLBT	TLITIA	TLHMOR
10	0.5170	0.3428	0.3428
11	0.1562	0.1030	0.1030
12	0.0460	0.0312	0.0312
13	0.0131	0.0093	0.0093
14	0.0036	0.0026	0.0026
15	9.9176×10^{-4}	7.1795×10^{-4}	7.1861×10^{-4}

within the desired time interval is compared in Figure 4.

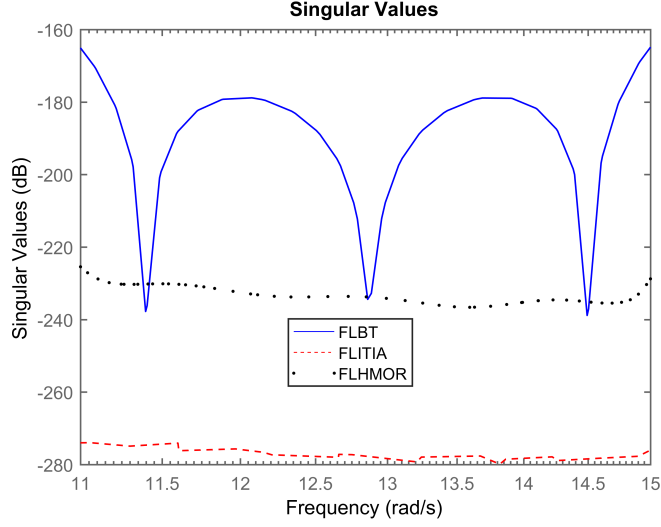


Figure 3.: Singular values of $E(s)$ within $[11, 15]$ rad/sec

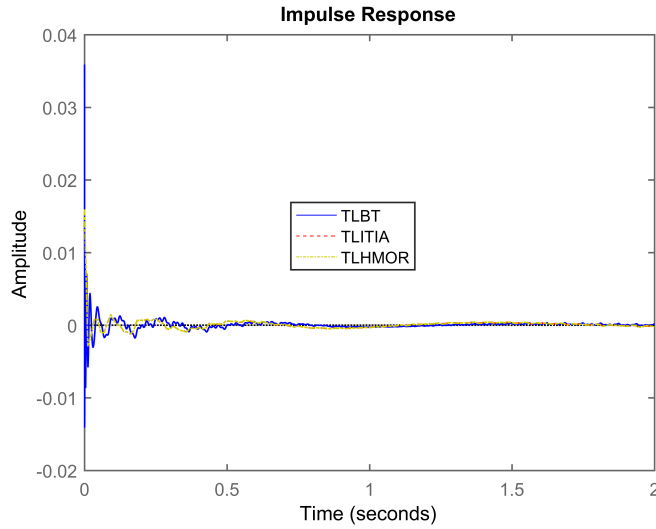


Figure 4.: Impulse response of $E(s)$ within $[0, 2]$ sec

7.5. International Space Station

Let us consider the 348th order international space station model as the test system from the benchmark collection of test systems for MOR, cf. (Chahlaoui and Van Dooren, 2005). This model has 3 inputs and 3 outputs. For the frequency-limited case, the desired frequency interval is chosen as $[-12, -9] \cup [9, 12]$ rad/sec. The international space station model is reduced by using FLBT, FLITIA, and FLHMOR, and their accuracy is compared in Table 6. It can be noticed that FLITIA and FLHMOR offer less $\|E(s)\|_{\mathcal{H}_{2,\omega}}$ than FLBT. There are 9 frequency-domain plots of the 3×3 error transfer function that are not shown for brevity. For the time-limited case, the desired time interval is chosen as $[0, 2.5]$ sec. The international space model is reduced

Table 6.: $\|E(s)\|_{\mathcal{H}_{2,\omega}}$

Order	FLBT	FLITIA	FLHMOR
15	3.4372×10^{-5}	2.4039×10^{-5}	2.4039×10^{-5}
16	2.7377×10^{-5}	1.1905×10^{-5}	1.1905×10^{-5}
17	5.1045×10^{-5}	1.0804×10^{-5}	1.0804×10^{-5}
18	5.1055×10^{-5}	3.6488×10^{-6}	3.6488×10^{-6}
19	5.0940×10^{-5}	3.4274×10^{-6}	3.4274×10^{-6}
20	2.8898×10^{-5}	2.9185×10^{-6}	2.9211×10^{-6}

by using TLBT, TLITIA, and TLHMOR, and their accuracy is compared in Table 7. It can be noticed that TLITIA and TLHMOR offer less $\|E(s)\|_{\mathcal{H}_{2,\tau}}$ than TLBT.

Table 7.: $\|E(s)\|_{\mathcal{H}_{2,\tau}}$

Order	TLBT	TLITIA	TLHMOR
15	9.5009×10^{-4}	5.8676×10^{-4}	5.8676×10^{-4}
16	6.3547×10^{-4}	5.1907×10^{-4}	5.1907×10^{-4}
17	3.8048×10^{-4}	3.6969×10^{-4}	3.6969×10^{-4}
18	5.6965×10^{-4}	4.2228×10^{-4}	4.2228×10^{-4}
19	2.5937×10^{-4}	1.9977×10^{-4}	1.9977×10^{-4}
20	1.8241×10^{-4}	1.7952×10^{-4}	1.7952×10^{-4}

There are 9 time-domain plots of the 3×3 error transfer function that are not shown for brevity.

8. Conclusion

The $\mathcal{H}_{2,\omega}$ - and $\mathcal{H}_{2,\tau}$ -optimal MOR problems within the oblique projection framework are addressed. It is shown that two out of three optimality conditions can be exactly satisfied within the oblique projection framework, whereas the third optimality condition can be nearly satisfied. The equivalence between gramian-based optimality conditions and the tangential interpolation conditions is also established. Two iterative tangential interpolation algorithms are proposed that nearly satisfy the three optimality conditions upon convergence. The deviations in satisfaction of the optimality conditions decay quickly as the order of the reduced model increases. Further, two stationary point iteration algorithms are proposed that exactly satisfy two optimality conditions upon convergence, while the third optimality condition is nearly satisfied. The deviation in satisfaction of the third optimality condition decays quickly as the order of the reduced model increases. The numerical results confirm that the proposed algorithms construct near-optimal ROMs, which exhibit high fidelity within the desired frequency and time intervals.

References

Astolfi, A., Scarciotti, G., Simard, J., Faedo, N., and Ringwood, J. V. (2020). Model reduction by moment matching: Beyond linearity a review of the last 10 years. In *2020 59th IEEE*

- Conference on Decision and Control (CDC)*, pages 1–16. IEEE.
- Beattie, C. A. and Gugercin, S. (2009). A trust region method for optimal \mathcal{H}_2 model reduction. In *Proceedings of the 48th IEEE Conference on Decision and Control (CDC) held jointly with 2009 28th Chinese Control Conference*, pages 5370–5375. IEEE.
- Beattie, C. A. and Gugercin, S. (2017). Model reduction by rational interpolation. *Model Reduction and Algorithms: Theory and Applications*, P. Benner, A. Cohen, M. Ohlberger, and K. Willcox, eds., *Comput. Sci. Engrg*, 15:297–334.
- Benner, P. (2018). *Model reduction of complex dynamical systems*. Springer Nature.
- Benner, P., Köhler, M., and Saak, J. (2011). Sparse-dense Sylvester equations in \mathcal{H}_2 -model order reduction. mpi magdeburg preprints mpimd/11-11, 2011.
- Benner, P., Kürschner, P., and Saak, J. (2016). Frequency-limited balanced truncation with low-rank approximations. *SIAM Journal on Scientific Computing*, 38(1):A471–A499.
- Benner, P., Mehrmann, V., and Sorensen, D. C. (2005). *Dimension reduction of large-scale systems*, volume 45. Springer.
- Castagnotto, A., Beattie, C., and Gugercin, S. (2017). Interpolatory methods for \mathcal{H}_∞ model reduction of multi-input/multi-output systems. In *Model Reduction of Parametrized Systems*, pages 349–365. Springer.
- Chahlaoui, Y. and Van Dooren, P. (2005). Benchmark examples for model reduction of linear time-invariant dynamical systems. In *Dimension reduction of large-scale systems*, pages 379–392. Springer.
- Du, X., Uddin, M. M., Fony, A. M., Hossain, M., Sahadat-Hossain, M., et al. (2021). Frequency limited \mathcal{H}_2 optimal model reduction of large-scale sparse dynamical systems. *arXiv preprint arXiv:2101.04566*.
- Du, X. and Yang, G.-H. (2010). \mathcal{H}_∞ model reduction of linear continuous-time systems over finite-frequency interval. *IET control theory & applications*, 4(3):499–508.
- Gallivan, K., Vandendorpe, A., and Van Dooren, P. (2004). Sylvester equations and projection-based model reduction. *Journal of Computational and Applied Mathematics*, 162(1):213–229.
- Gawronski, W. and Juang, J.-N. (1990). Model reduction in limited time and frequency intervals. *International Journal of Systems Science*, 21(2):349–376.
- Goyal, P. and Redmann, M. (2019). Time-limited \mathcal{H}_2 -optimal model order reduction. *Applied Mathematics and Computation*, 355:184–197.
- Grimme, E. J. (1997). *Krylov projection methods for model reduction*. University of Illinois at Urbana-Champaign.
- Gugercin, S. (2008). An iterative SVD-Krylov based method for model reduction of large-scale dynamical systems. *Linear Algebra and its Applications*, 428(8-9):1964–1986.
- Gugercin, S., Antoulas, A. C., and Beattie, C. (2008). \mathcal{H}_2 model reduction for large-scale linear dynamical systems. *SIAM journal on matrix analysis and applications*, 30(2):609–638.
- Gugercin, S., Sorensen, D. C., and Antoulas, A. C. (2003). A modified low-rank Smith method for large-scale Lyapunov equations. *Numerical Algorithms*, 32(1):27–55.
- Ibrir, S. (2018). A projection-based algorithm for model-order reduction with \mathcal{H}_2 performance: A convex-optimization setting. *Automatica*, 93:510–519.
- Kürschner, P. (2018). Balanced truncation model order reduction in limited time intervals for large systems. *Advances in Computational Mathematics*, 44(6):1821–1844.
- Li, J.-R. and White, J. (2002). Low rank solution of Lyapunov equations. *SIAM Journal on Matrix Analysis and Applications*, 24(1):260–280.
- Li, X., Yu, C., and Gao, H. (2014). Frequency-limited \mathcal{H}_∞ model reduction for positive systems. *IEEE Transactions on Automatic Control*, 60(4):1093–1098.
- Penzl, T. (1999). A cyclic low-rank Smith method for large sparse Lyapunov equations. *SIAM Journal on Scientific Computing*, 21(4):1401–1418.
- Petersson, D. (2013). *A nonlinear optimization approach to \mathcal{H}_2 -optimal modeling and control*. PhD thesis, Linköping University Electronic Press.
- Petersson, D. and Löfberg, J. (2014). Model reduction using a frequency-limited \mathcal{H}_2 -cost. *Systems & Control Letters*, 67:32–39.

- Quarteroni, A., Rozza, G., et al. (2014). *Reduced order methods for modeling and computational reduction*, volume 9. Springer.
- Schilders, W. H., Van der Vorst, H. A., and Rommes, J. (2008). *Model order reduction: theory, research aspects and applications*, volume 13. Springer.
- Sinani, K. and Gugercin, S. (2019). $\mathcal{H}_2(tf)$ optimality conditions for a finite-time horizon. *Automatica*, 110:108604.
- Tahavori, M. and Shaker, H. R. (2013). Model reduction via time-interval balanced stochastic truncation for linear time invariant systems. *International Journal of Systems Science*, 44(3):493–501.
- Van Dooren, P., Gallivan, K. A., and Absil, P.-A. (2008). \mathcal{H}_2 -optimal model reduction of MIMO systems. *Applied Mathematics Letters*, 21(12):1267–1273.
- Vuillemin, P. (2014). *Frequency-limited model approximation of large-scale dynamical models*. PhD thesis, ISAE-Institut Supérieur de l’Aéronautique et de l’Espace.
- Vuillemin, P., Poussot-Vassal, C., and Alazard, D. (2013). \mathcal{H}_2 optimal and frequency limited approximation methods for large-scale lti dynamical systems. *IFAC Proceedings Volumes*, 46(2):719–724.
- Wilson, D. (1970). Optimum solution of model-reduction problem. In *Proceedings of the Institution of Electrical Engineers*, volume 117, pages 1161–1165. IET.
- Wolf, T. (2014). \mathcal{H}_2 pseudo-optimal model order reduction. PhD thesis, Technische Universität München.
- Wolf, T., Panzer, H. K., and Lohmann, B. (2013). \mathcal{H}_2 pseudo-optimality in model order reduction by Krylov subspace methods. In *2013 European control conference (ECC)*, pages 3427–3432. IEEE.
- Xu, Y. and Zeng, T. (2011). Optimal \mathcal{H}_2 model reduction for large scale MIMO systems via tangential interpolation. *International Journal of Numerical Analysis & Modeling*, 8(1).
- Zhou, K., Doyle, J., and Glover, K. (1996). Robust and optimal control. *Control Engineering Practice*, 4(8):1189–1190.
- Zulfiqar, U., Sreeram, V., and Du, X. (2019). Adaptive frequency-limited \mathcal{H}_2 -model order reduction. *arXiv preprint arXiv:1911.11427*.
- Zulfiqar, U., Sreeram, V., and Du, X. (2020a). Frequency-limited pseudo-optimal rational Krylov algorithm for power system reduction. *International Journal of Electrical Power & Energy Systems*, 118:105798.
- Zulfiqar, U., Sreeram, V., and Du, X. (2020b). Time-limited pseudo-optimal \mathcal{H}_2 -model order reduction. *IET Control Theory & Applications*, 14(14):1995–2007.